# THE AMERICAN MINERALOGIST

JOURNAL OF THE MINERALOGICAL SOCIETY OF AMERICA

Vol. 27 AUGUST, 1942 No. 8

THE RARE ALKALIES IN MICAS*

R. E. STEVENS AND W. T. SCHALLER,
Geological Survey, Washington, D. C.

CONTENTS

ABSTRACT

Determinations are given of all of the alkalies (lithium, sodium, potassium, rubidium, and cesium) in 43 samples of micas, including paragonite, muscovite, biotite, phlogopite, vermiculite, zinnwaldite, taeniolite, lepidolite, and polylithionite.

The geologic occurrence of the rare alkalies in micas is discussed. Increase in rare alkalies in micas from successive stages of hydrothermal replacement in pegmatites is shown. Lithium was found to be present in all the micas analyzed, but rubidium and cesium were found only in micas from the later stages of magmatic differentiation.

INTRODUCTION

This study is the first of a projected series on the geologic occurrence of the rare alkalies—lithium, rubidium, and cesium. Some micas, particularly those in pegmatites, are known to contain the rare alkalies and further analyses of micas will give additional information of the way the rare alkalies are concentrated in nature. The three rare alkalies are very seldom determined in the analyses of rocks or minerals and hence very little is known about their distribution. As a preliminary step in the analysis of some micas containing rare alkalies, the methods of separating and determining all five alkalies were studied by Wells and Stevens and a satisfactory procedure was developed.[1] On the basis of these improved

* Published by permission of the Director, Geological Survey, Washington, D. C.

[1] Wells, Roger C., and Stevens, Rollin E., Determination of the common and rare alkalies in mineral analysis: *Ind. & Eng. Chem.*, Anal. Ed., **6**, 439 (1934).

methods, it is planned to make analyses of various mineral groups, such as the micas, the feldspars, the beryls, and others. As a first contribution, the five alkalies have been determined in a suite of micas and the results obtained are here presented. It is realized fully that the series is incomplete and it is hoped that further determinations will help to complete the picture.

The data here presented were determined for 3 paragonites, 12 muscovites, 6 biotites, one phlogopite, one taeniolite, one zinnwaldite, one vermiculite and 18 lepidolites (including polylithionite). The results for the paragonites, lepidolites, two biotites, and for taeniolite and zinnwaldite have already been published in the descriptions of these minerals. The analyses are listed under each mineral name in the order of increasing percentages of Li_2O. The analyses were made by Stevens and the collection and preparation of most of the samples and discussion of the geochemical relations is by Schaller.

Paragonite

The alkalies in three paragonites[2] are shown in Table 1.

Table 1. Alkalies in Paragonite

	1. Switzerland	2. Italy	3. Euphyllite, Pennsylvania
Li_2O	0.08	0.13	0.73
Na_2O	6.28	7.26	5.64
K_2O	2.17	1.01	1.71
Rb_2O	0.12	None	0.11
Cs_2O	None	None	None

1. Monte Campione, Switzerland.
2. Fenestrella, near Borgofranco, Valle del Chisone, Piedmont, Italy.
3. Corundum Hill, Pa.

All three samples contain lithium; rubidium is present in very small quantities in two samples and absent in one, and cesium is absent in all three samples.

Muscovite

Eleven of the twelve muscovites are from pegmatites, nine from San Diego County, California.

[2] Schaller, W. T., and Stevens, R. E., The validity of paragonite as a mineral species: *Am. Mineral.*, **26**, 541–545 (1941).

TABLE 2. ALKALIES IN MUSCOVITE

	1. N.C.	2. Calif.	3. Tyrol	4. Calif.	5. Calif.	6. Calif.
Li_2O	0.04	0.05	0.07	0.07	0.19	0.28
Na_2O	0.72	0.83	1.81	0.92	0.78	0.81
K_2O	10.59	10.21	8.89	9.90	10.26	10.05
Rb_2O	None	0.12	None	None	0.08	0.17
Cs_2O	None	0.11	None	None	0.03	0.12
	7. Calif.	**8. Calif.**	**9. Calif.**	**10. N.M.**	**11. Calif.**	**12. Calif.**
Li_2O	0.31	0.33	0.36	0.38	0.47	0.55
Na_2O	0.86	1.06	0.85	0.91	0.76	0.45
K_2O	10.13	9.97	10.27	10.07	10.30	11.06
Rb_2O	None	0.25	0.12	0.82	None	0.08
Cs_2O	None	0.17	0.08	0.09	None	0.14

1. Ordinary commercial sheet mica, pale olive in color. From Spruce Pine area, N. C. Sent in by B. C. Burgess of Spruce Pine. Relatively high in iron. Material analyzed, carefully separated from included visible iron oxides, contains 1.42 per cent FeO and 4.38 per cent Fe_2O_3, as determined by J. G. Fairchild.

2. Granular mass of greenish mica associated with abundant almandine garnet. A.B.C. gem mine, Ramona, San Diego County, Calif.

3. Medium grained, resembling coarse sericite schist. Pregratten, Pusterthal, Tyrol. Labeled paragonite, var. pragrattite. U. S. Nat. Mus. Coll. No. R4415.

4. Parallel blades of muscovite intergrown with albitized pegmatite. Victor gem mine, Rincon, San Diego County, Calif.

5. Plumose muscovite in microcline graphic granite at edge of albitized area. North end of Douglas dike (below the Stewart mine), at east base of Stewart Hill, Pala, San Diego County, Calif. Although occurring in microcline graphic granite, adjacent to albitized pegmatite, the muscovite definitely belongs to the sodium phase of replacement, the development of the muscovite and associated black tourmaline advancing slightly beyond the zone of formation of abundant albite. The non-albitized microcline and microcline graphic granite of the pegmatites not adjacent to an albitized zone are essentially free from any muscovite.

6. Small sheets of greenish muscovite, 2 to 3 inches across, with narrow border of lepidolite. The lepidolite and half inch of adjoining muscovite removed. Ed. Fletcher gem mine, north side of Stewart Hill, Pala, San Diego County, Calif.

7. Sheets of muscovite in pegmatite, largely albitized. Mission gem mine, near southern base of Stewart Hill, Pala, San Diego County, Calif.

8. Small sheets of muscovite, intergrown with crystals of albite, Pala View gem mine, on southeastern slope of Stewart Hill (above the Stewart mine), Pala, San Diego County, Calif. U. S. Nat. Mus. Coll. No. 89,190. The muscovite shows poorly developed crystal faces and the specimen evidently came from a cavity.

9. Small sheets of greenish muscovite, 2 inches long and 1 to $1\frac{1}{2}$ inches wide, with narrow border of lepidolite. The lepidolite border and quarter inch of adjoining muscovite removed. Hiriart gem mine, Hiriart Hill, Pala, San Diego County, Calif.

10. Purple muscovite from Harding mine, about 10 miles east of Embudo, Taos County, New Mexico. Description of purple muscovite published by Schaller, W. T., and Henderson, E. P., Purple muscovite from New Mexico: *Am. Mineral.*, **11**, 5–16 (1926).

11. Sheets of muscovite, about one half inch wide, in albitized pegmatite. From south end of Douglas dike (below Stewart mine) on southeastern base of Stewart Hill, Pala, San Diego County, Calif.

12. Compact, fine-grained sericite. In pegmatite of Labat's gem mine, N.E. of Warner Hot Springs, San Diego County, Calif.

The purple muscovite from the Harding mine, New Mexico, is considerably richer in the rare alkalies than any sample of muscovite from San Diego County, Calif. The compact sericite (no. 12) from Labat's gem mine contains more rare alkalies than any of the sheet muscovites, even those (nos. 6 and 9) with a border of lepidolite.

Lithium is present in every muscovite analyzed. Both rubidium and cesium are present in seven of the twelve samples. Their quantity, however, is small in the samples from California. There seems to be no obvious relation between the quantity of lithium and the combined quantities of rubidium and cesium.

Biotite

Six biotites were analyzed for rare alkalies, five from pegmatites and one from the Alberene quarry, Virginia. In these biotites, the percentage of FeO, MnO, and MgO, where determined, are added to help characterize the biotites.

Table 3. Alkalies in Biotite

	1. Va.	2. Va.	3. S.D.	4. Calif.	5. Calif.	6. N.C.
Li_2O	0.09	0.11	0.65	1.05	1.17	1.20
Na_2O	0.22	0.86	0.45	0.22	0.19	0.73
K_2O	9.54	8.08	8.48	8.47	8.80	8.54
Rb_2O	None	None	1.48	0.10	0.08	1.85
Cs_2O	None	None	1.12	0.08	0.14	0.47
FeO	N.d.	8.96	14.81	13.89	24.21	8.29
MnO	N.d.	0.24	0.22	N.d.	N.d.	0.27
MgO	N.d.	16.15	8.45	N.d.	N.d.	9.55

1. Black mica from the Alberene Quarry, Alberene, Albermarle County, Virginia. Sample furnished by C. S. Ross.

2. Black mica from the contact of simple pegmatite (free from lithium minerals) and schist. The pegmatite was formerly mined for commercial sheet muscovite. Ridgway, Virginia. Collected by W. T. Schaller. Mica completely analysed by R. E. Stevens.

3. Brown mica from pegmatite on property of Maywood Chemical Co., 8 miles N.W. of Custer, South Dakota. Described by Hess, F. L., and Fahey, J. J., Cesium biotite from Custer County, South Dakota: *Am. Mineral.*, **17**, 173–176 (1932), with corrections of percentages of potassium, rubidium, and cesium, by Hess, F. L., and Stevens, R. E., A rare-alkali biotite from Kings Mountain, North Carolina: *Am. Mineral.*, **22**, 1044 (1937).

4. Black mica from top of upper part of pegmatite at S.W. end of Tourmaline Queen gem mine, eastern side of Stewart Hill, Pala, San Diego County, Calif. Iron determination by J. J. Fahey.

5. Greenish mica from Panama Pacific Exposition gem mine, Chihuahua Valley, San Diego County, California. Iron determinations by J. J. Fahey.

6. Brown mica from spodumene carrying pegmatite at Kings Mountain, North Carolina. Described by Hess, F. L., and Stevens, R. E., A rare-alkali biotite from Kings Mountain, North Carolina: *Am. Mineral.*, **22**, 1040 (1937).

All six biotites contain lithium in greater quantity than the muscovites. Four of the biotites contain more lithium than the lithium richest muscovite; three of the biotites have twice as much as the lithium richest muscovite. The average of the six biotites (0.71 per cent Li_2O) is nearly three times as much as the average of the 12 muscovites (0.26 per cent Li_2O). Rubidium and cesium, as in the muscovites, are present in some and absent in others. Their quantity in samples nos. 3 and 6, from pegmatites containing abundant lithium minerals, equals the quantity in the lepidolites. The percentage of Rb_2O+Cs_2O in either of these two biotites exceeds that of any of the 18 lepidolites listed and the average (2.46 per cent) exceeds considerably the average (1.57) of the 18 lepidolites. The average of the five biotites from pegmatites (1.06 per cent) is five times that of the average (0.20 per cent) of the 12 muscovites. As was to be expected, the biotite (no. 1) from the soapstone quarry at Alberene, Va., contained neither rubidium nor cesium. Their absence in the biotite (no. 2) from Ridgeway, Va., however, was unexpected, as the zinnwaldite from Amelia, Va., contains appreciable rubidium and some cesium, although other lithium minerals are not known to be present in either pegmatite.

The average per cent of Na_2O (0.45) in the biotites is only half as great (0.90) as that in the muscovites.

Phlogopite, Vermiculite, Zinnwaldite and Taeniolite

The rare alkalies were determined in only one sample of each of these micas.

Table 4. Alkalies in Phlogopite, Vermiculite, Zinnwaldite, and Taeniolite

	Phlogopite	Vermiculite	Zinnwaldite	Taeniolite
Li_2O	0.05	0.04	1.92	3.10
Na_2O	0.35	0.20	0.74	0.64
K_2O	10.14	2.66	9.56	10.44
Rb_2O	None	None	1.04	None
Cs_2O	None	0.02	0.10	None

Phlogopite. From Cockeysville marble, north of Baltimore, Md. Sample furnished by C. S. Ross.

Vermiculite. Yellow Mt., Macon County, Georgia. Alkalies by Wells and Stevens.

Zinnwaldite. Morefield mine, Amelia, Amelia County, Virginia. Analysis of mica by J. J. Fahey, cesium by Stevens, and other alkalies by Wells. Described by Glass, J. J., The pegmatite minerals from near Amelia, Virginia: *Am. Mineral.*, **20,** 756 (1935).

Taeniolite. Magnet Cove, Arkansas. Described by Miser, H. D., and Stevens, R. E., Taeniolite from Magnet Cove, Arkansas: *Am. Mineral.*, **23,** 104–110 (1938).

Lepidolite, Including Polylithionite

Samples nos. 1 to 4 and 5 to 17, and the localities are described by Stevens.[3] No. 4*a*, fine-grained lepidolite appearing pale greenish in the matrix, was furnished by Prof. H. Mohr of the Deutsche Technische Hochschule at Brno, Czechoslovakia. This greenish lepidolite, much less abundant at Rožna than the more common lilac colored variety, was stated[4] to contain only 1.78 per cent Li_2O, but Stevens found 3.90 per cent. No. 17 is polylithionite from Greenland and nos. 15 (from Ramona, Calif.) and 16 (from Madagascar) approach polylithionite.

Lepidolite no. 1 from Manitoba, Canada, and the relatively low lithium samples from the Stewart mine, Pala, California, have the muscovite type of structure, according to Hendricks,[5] and should probably be called muscovite rather than lepidolite.

All of these lepidolites, except no. 17 (polylithionite from Greenland), are from typical granitic pegmatites and show no relation between the quantity of rubidium and cesium, and their geographic distribution. Rubidium exceeds cesium in every analysis though the two alkalies are present in nearly equal quantities in sample no. 9 from the San Diego mine at Mesa Grande, but in the two samples (nos. 8 and 13) from the adjoining Himalaya mine, on the northward extension of the same pegmatite dike, rubidum greatly exceeds cesium. Neither is there any relation between lithium as compared with rubidium and cesium, either for all the lepidolites or for those from different parts of a single dike. Compare, for example, nos. 3, 5, 6, 11, and 12 from the Stewart mine at Pala and nos. 8, 9, and 13 from Mesa Grande. Neither polylithionite from Greenland (no. 17) nor taeniolite from Arkansas contain any cesium although rubidium is present in polylithionite and absent in taeniolite. Neither of these two minerals are from typical granitic pegmatites, and although the taeniolite occurs in chert (novaculite), it is on the border of the nepheline rich rocks of Magnet Cove from which the lithium, fluorine, potassium, and magnesium apparently were derived.

[3] Stevens, R. E., New analyses of lepidolites and their interpretation: *Am. Mineral.*, **23,** 615 (1938).

[4] Mohr, H., Das Lepidolitvorkommen "Rožna" in Mähren als Lithiumerz-Lagerstätte: *Berg.- und Hüttenmännisches Jahrb.*, **82,** Heft 2, 48 (1934).

[5] Hendricks, S. B., Polymorphism of the micas: *Am. Mineral.*, **24,** 759–761, (1939), and personal communication.

Table 5. Alkalies in Lepidolite, including Polylithionite

	1	2	3	4	4a	5	6	7	8
Li_2O	2.70	3.51	3.70	3.81	3.90	3.96	5.04	5.05	5.11
Na_2O	0.77	1.27	0.87	0.64	0.95	0.77	0.74	0.57	0.57
K_2O	9.52	10.32	10.02	9.91	10.13	9.93	9.58	10.14	9.53
Rb_2O	1.93	1.11	0.91	1.55	1.39	1.56	1.56	1.62	1.64
Cs_2O	0.18	0.13	0.16	0.11	0.17	0.12	0.48	0.09	0.17
	9	10	11	12	13	14	15	16	17
Li_2O	5.33	5.39	5.51	5.64	5.78	5.89	6.18	6.84	7.26
Na_2O	0.89	0.59	0.63	0.59	0.65	0.82	0.72	0.44	0.53
K_2O	10.79	10.14	10.25	10.11	9.90	9.70	10.28	10.65	11.05
Rb_2O	0.42	0.97	1.38	1.04	2.00	1.38	1.22	1.35	1.14
Cs_2O	0.41	0.06	0.48	0.67	0.08	0.09	0.24	0.40	None

1. Manitoba, Canada.
2, 3, 5, 6, 11, 12. Pala, Calif.
4. Chihuahua Valley, San Diego County, Calif.
4a. Mt. Hradiska, Rožna, Moravia, Czechoslovakia.
7. Ohio City, Colorado.
8, 9, 13. Mesa Grande, Calif.
10. Wakefield, Canada.
14. W. Australia.
15. Ramona, Calif.
16. Madagascar.
17. Greenland.

Distribution of Rare Alkalies in Different Micas

The distribution of the rare alkalies in the different micas analyzed may be shown by the average values for the four named micas, paragonite, muscovite, biotite, and lepidolite.

Table 6. Average Percentage of Rare Alkalies in Paragonite, Muscovite, Biotite and Lepidolite

	Paragonite	Muscovite	Biotite	Lepidolite
Li_2O	0.31	0.26	0.71	4.90
Rb_2O	0.08	0.14	0.59	1.35
Cs_2O	0.00	0.06	0.30	0.24
Total	0.39	0.46	1.60	6.49

These average values must be considered as applying only to the samples analyzed and possibly not to these four micas in general, for which

data on the content of rare alkalies are woefully lacking. Furthermore, the micas analyzed were largely pegmatitic micas, namely, one of the three paragonites, eleven of the twelve muscovites, five of the six biotites, and all of the eighteen lepidolites.

Average values may also be given on the basis of type of occurrence, as non-pegmatitic and pegmatitic.

TABLE 7. AVERAGE PERCENTAGE OF RARE ALKALIES IN NON-PEGMATITIC MICAS AND PEGMATITIC MICAS

	7 Non-pegmatitic micas		18 Pegmatitic micas, excluding lepidolites	35 Pegmatitic micas, including lepidolites
	Excluding taeniolite	Including taeniolite		
Li_2O	0.08	0.51	0.55	2.66
Rb_2O	0.02	0.02	0.35	0.84
Cs_2O	0.00	0.00	0.15	0.19
Total	0.10	0.53	1.05	3.69

The seven non-pegmatitic micas include the two paragonites (nos. 1 and 2) from Switzerland and Italy, one muscovite (no. 3) from the Tyrol, one biotite (no. 1) from Alberene, Virginia, phlogopite, vermiculite, and taeniolite. The average values for the non-pegmatitic micas are given with taeniolite excluded and included, as the 3.10 per cent of Li_2O in taeniolite raises the average per cent considerably. Only one of these non-pegmatitic micas (paragonite no. 1) contains rubidium (0.12 per cent Rb_2O) and only one (vermiculite, with 0.02 per cent Cs_2O) contains any cesium. Of the eighteen pegmatitic micas, excluding lepidolite, only five contain no rubidium and only six contain no cesium. All the seventeen lepidolites (not including the polylithionite from Greenland, which contains rubidium but no cesium) contain both rubidium and cesium.

INCREASE IN PERCENTAGES OF RARE ALKALIES IN PEGMATITES WITH SUCCESSIVE STAGES OF HYDROTHERMAL REPLACEMENT

Muscovite is the only one of these micas for which a small suite of samples from known stages of successive hydrothermal replacement in pegmatites could be obtained. These samples were prepared from specimens from the southern California field of lithium-bearing pegmatites. If the theory[6] is correct that these pegmatites originally consisted only

[6] Schaller, W. T., The genesis of lithium pegmatites: *Am. Jour. Sci.*, ser. 5, **10**, 269–279 (1925).

of feldspars with possibly some quartz, then all micas now present are later and have been introduced in successive stages of hydrothermal replacements. Accumulating evidence shows the general soundness of the replacement theory. In general, two main successive stages of hydrothermal replacement may be defined, for the present purpose, as follows:

(1) Sodium stage, A. Albitization. Development of large quantities of albite with minor associated muscovite, garnet and black tourmaline, by replacement of the primary microcline and microcline graphic granite. The resulting albitized pegmatite is solid rock, almost free from any cavities lined with terminated crystals. Where such small cavities exist in the albitized rock, as they do very occasionally, it is believed that the rock has been subjected to the beginning of the second stage.

(2) Lithium stage, B. Development of large quantities of lepidolite and green and pink lithium tourmaline. At some places, lithium minerals have developed extensively without the formation of any cavities, as for example the large lenses containing thousands of tons of massive lepidolite at the Stewart mine at Pala. At other places, cavities have developed to a considerable extent, with well crystallized terminated minerals, as at Mesa Grande.

Five (nos. 2, 4, 5, 7, and 11) of the muscovites from the California pegmatites, for which the percentages of alkalies present have been determined, are from the sodium or albitization stage. The content of rare alkalies in these muscovites is shown in Table 8 under A. Three (nos. 6, 8, and 9) of the muscovites from the California pegmatites are from the beginning of the lithium stage, as shown by the presence of the lepidolite borders (nos. 6 and 9) or by cavities (no. 8).

In the full development of the lithium stage, the mica formed is essentially lepidolite. No new muscovite is formed in this stage. The muscovite now present in specimens from the lithium phase is residual muscovite from the preceding sodium phase, as evidenced by the many examples of muscovite completely or partially changed to lepidolite, by the pink color of this muscovite with percentages of Li_2O intermediate between those of the greenish muscovites of the albite phase and those of lepidolite,[7] and by the border of lepidolite formed around the muscovite, which is often colored pink adjacent to the lepidolite border. The content

[7] The pink muscovite from pegmatites from various localities in the world are similar examples, such as the purple muscovite from New Mexico (muscovite no. 10), the rose-colored mica from Goshen, Mass., with 0.64 percent Li_2O, the several lilac or gray muscovites from Manitoba, described by Ellsworth, H. V. (Rare-element minerals from Canada, Geol. Survey, *Econ. Geol.* Ser., no. **11**, 264–266, 1932), with from 0.90 to 1.80 per cent Li_2O, and the rose-colored muscovites from Sweden (Berggren, Thelma, Minerals of the Varuträsk pegmatite. XV. Analyses of mica minerals and their interpretation: *Geol. Fören. Stockholm Föhr.*, **62**, heft 2, 185, 1940), with from 0.69 to 1.10 per cent Li_2O.

of rare alkalies in these muscovites of the beginning of the lithium stage is shown in Table 8 under B.

TABLE 8. RARE ALKALIES IN MUSCOVITES FROM CALIFORNIA PEGMATITES ARRANGED IN TWO STAGES OF HYDROTHERMAL REPLACEMENTS

	Sodium stage, A						Beginning of lithium stage, B			
	In microcline graphic granite	In albitized pegmatite					With border of lepidolite		Cavity	
	5	2	4	7	11	Av.	6	9	8	Av.
Li_2O	0.19	0.05	0.07	0.31	0.47	0.22	0.28	0.36	0.33	0.32
Rb_2O	0.08	0.12	0.00	0.00	0.00	0.04	0.17	0.12	0.25	0.18
Cs_2O	0.03	0.11	0.00	0.00	0.00	0.03	0.12	0.08	0.17	0.12
Total	0.30	0.28	0.07	0.31	0.47	0.29	0.57	0.56	0.75	0.62

The position of the compact sericite (muscovite no. 12) from Labat's gem mine, California, in the hydrothermal replacement series, is unknown. From its location in the pegmatite it was thought to be related to the early sodium or albitization stage (A), but its relatively high content of rare alkalies suggests that it is related to the beginning of the lithium stage (B). Similarly, the oncosine (crypto-crystalline muscovite or sericite) from Varuträsk[8] contains more lithium and cesium than do the three muscovites for which analyses are given, though it is lower in rubidium.

The increase of rare alkalies in progressive stages of hydrothermal replacements in pegmatites is further shown in Table 9 by a comparison of certain average values. In column 1 are given the average percentages of the rare alkalies in eight micas,[9] chiefly from non-pegmatitic sources, or from pegmatites where hydrothermal replacements have played only a very minor part. Six of these eight samples contain neither rudibium nor cesium. The average percentages of the rare alkalies in the sodium phase (A) of the early hydrothermal replacement (chiefly albitization with accompaniment of minor quantities of muscovite, black tourmaline, and reddish-brown garnet), are shown in column 2, those in the begin-

[8] Berggren, *op. cit.*, p. 185, Analysis F.

[9] The two non-pegmatitic paragonites, the commercial sheet muscovite (no. 1) from a pegmatite at Spruce Pine, N. C., the non-pegmatitic muscovite (no. 3) from the Tyrol, biotite (no. 1) from Alberene, Va., biotite (no. 2) from a non-lithium pegmatite at Ridgeway, Va., phlogopite, and vermiculite.

ning of the lithium phase in column 3, and those in the full development of the lithium phase, culminating in lepidolite, in column 4. The increase in lithium and rubidium, although progressively irregular, is much greater than that of cesium.

Table 9. Increase in Percentages of Rare Alkalies in Micas from Various Stages of Replacement

	1	2	3	4
	Chiefly non-pegmatitic	Sodium phase, A, albitization	Beginning of lithium phase	Lithium phase, B
Li_2O	0.08	0.22	0.32	4.90
Rb_2O	0.01	0.04	0.18	1.35
Cs_2O	0.00	0.03	0.12	0.24
Total	0.09	0.29	0.62	6.49

The pegmatitic muscovite from North Carolina (no. 1, Table 2) and that from the Tyrol (no. 3) are free from[10] both rubidium and cesium, as are also three of the five muscovites from the first stage of albitization, suggesting that muscovites not from a later replacement stage contain neither rubidium nor cesium.

The average total rare alkali content, chiefly lithium, of the eight micas largely of non-pegmatitic sources, as given in column 1 of Table 9, is 0.09 per cent. That of the five muscovites (nos. 2, 4, 5, 7, 11) from the cavity free albitization stage of pegmatites, given in column 2, is 0.29 per cent, about three times as great as that for largely non-pegmatitic micas. This total quantity of rare alkalies, however, is still small. That is, the first stage of the albitization of the microcline and of microcline graphic granite in pegmatites, with its concomitant development of muscovite, garnet, and black tourmaline, was not accompanied by any noteworthy increase of the rare alkalies. The absence of any rubidium and cesium in three out of the five muscovites from albitized pegmatites of the sodium stage (A) is striking. Whether the quantities of the rare alkalies in the muscovites of stage A of the replacement series are about the same as, or greater than, the rare alkali content of the original replaced microcline, cannot be told until the analyses of such microclines are completed.

With the beginning of the lithium stage, the percentage of rare alkalies (av. = 0.62) is doubled over that of the sodium stage (av. = 0.29). The increase in rubidium and cesium however is much greater than that of

[10] That is "free from" in the sense that they could not be determined analytically.

lithium, which shows only a fifty per cent increase, whereas both rubidium and cesium increase about fourfold. The single sample of muscovite (no. 8) from a cavity and hence late, contains more of the rare alkalies than either of the two muscovites (nos. 6 and 9) with a border of lepidolite.

The later lithium stage of replacement with the development of much lepidolite is distinguished by considerable quantities of the rare alkalies, as evidenced by the analyses of the lepidolites. As shown by column 4, the quantity of Li_2O, in micas of the lithium phase (B) is 22 times that in the sodium phase (A), Rb_2O is 34 times, and Cs_2O is 8 times as much.

General Conclusions

It is realized fully that a consideration of the distribution of the rare alkalies lithium, rubidium, and cesium in micas, though based on analyses of 43 samples, is necessarily incomplete, and further investigations may not support some of the general tentative conclusions here expressed. The common micas (muscovite and biotite) in granitic rocks, in mica schists, in volcanic rocks, etc., have not been analyzed for their content of rare alkalies and the micas in metamorphic limestones are represented by only one sample.

Based only on the determinations here presented lithium seems to be present in every mica; at least it is found to be present in every mica for which a careful determination of lithium is made. If a "trace" be defined as not greater than 0.01 per cent in careful analytical work, the smallest quantities of Li_2O found (0.04 per cent in muscovite no. 1 and in vermiculite, 0.05 per cent in muscovite no. 2 and in phlogopite) are greater than "traces." Many mineral analyses report traces of lithium (in beryls for example) where the quantity may be much greater and as much as several tenths of a per cent. There is more lithium in pegmatitic biotites than in pegmatitic muscovites though the biotites have only half as much soda. The three analyses of the sodium mica paragonite show widely varying quantities of lithium. The element lithium is by no means restricted to minerals from pegmatites and if looked for will probably be found in many minerals not occurring in pegmatites. The magnesium clay from Hector, Calif., contains it as do several (if not all) margarites. The lithium-bearing taeniolite from Arkansas occurs in chert, and some manganese minerals contain lithium. Rubidium and cesium, on the other hand, seem to be restricted to pegmatitic minerals, judging from the very meager results available.

Rubidium is not known to occur as an essential constituent of any mineral. It is found in pegmatite minerals containing potassium such as the micas. However, not all pegmatite micas contain rubidium. It is

absent in the one sample of commercial sheet muscovite from North Carolina, in three muscovites (nos. 4, 7, and 11) from the gem pegmatites of San Diego County, Calif., and in the biotite from Ridgeway, Va. It occurs in the greatest quantity in those micas from the complex pegmatites which contain an abundance of lithium minerals although there is no relation as to its quantity as compared with the quantity of lithium in any single mineral. In general, it seems to be absent in non-pegmatitic micas. Thus the biotite from the soapstone area at Alberene, Va., and the phlogopite from the Cockeysville marble near Baltimore, Md., are free from rubidium yet the paragonite schist with kyanite from Monte Campino, Switzerland, has 0.12 per cent Rb_2O. It occurs most abundantly in the lepidolites, reaching a maximum of two per cent Rb_2O in lepidolite no. 13.

Cesium generally accompanies rubidium in the micas though generally in much smaller amounts. Only in muscovite no. 12 and in biotite no. 5, both from California, does the percentage of Cs_2O exceed that of Rb_2O. Cesium is absent in all three paragonites, in five muscovites, which are also free from rubidium, in two biotites, and in phlogopite and taeniolite, likewise free from rubidium. The small quantity of 0.02 per cent Cs_2O, with no rubidium, in the vermiculite from Georgia, is unusual. Cesium is absent in polylithionite but present in all the lepidolites. Its occurrence in micas seems to bear no relation to the quantity of either lithium or rubidium present.

One can only conclude from these results that the distribution of the rare alkalies lithium, rubidium, and cesium is very erratic in any single pegmatite, and in pegmatites in general, as illustrated by the development of the only cesium mineral, pollucite, with relatively very little lithium and rubidium in pegmatites from Elba, Maine, South Dakota, and Sweden. The three rare alkalies are just as erratic in any given mica but their total quantity increases with the successive stages of hydrothermal replacement.

NOMOGRAMS OF OPTIC ANGLE FORMULAE*

JOHN B. MERTIE, JR.,
U. S. Geological Survey, Washington, D. C.

ABSTRACT

Nomograms are presented herewith for the solution of several well-known petrographic formulae that are used in the measurement of optic angles. To solve for any one of the four variables α, β, γ, and V, when three of them are known, a grid type nomogram has been prepared; and a similar chart has been drawn to show the relationships between the variables α, β, γ, and E. Two nomograms are also presented for the solution of the equations $\sin E=\beta \sin V$ and $D=K \sin E$ (Mallard's formula). The method of preparing these charts is outlined, and their uses given. The topic of errors in observations and in computations is also considered.

INTRODUCTION

The equations that give the true and apparent optic angles of a biaxial mineral, as functions of its three indices of refraction, are well known to petrographers. But these equations contain four variables, and cannot be represented by single graphs, using ordinary two-dimensional Cartesian or polar coordinates. A graphic solution of an equation that relates approximately the variables V, α, β, and γ was published by Wright, who utilized a combination of Cartesian and polar coordinates; but the use of this chart requires a preliminary subtraction of α from β, and of α from γ, in order to obtain an equation containing only three variables. Later Wright published three similar graphs, charting both the approximate and true equations, but these likewise required preliminary arithmetical work between the variables α, β, and γ, and were therefore essentially three variable charts. In more recent years, Smith published a graph for obtaining the value of V, when α, β and γ are known, charting an approximation formula similar to the one charted by Wright. This graph uses one or more moving calibrated scales, and requires a threefold visual interpolation. Still later, Lane and Smith published another graph of the same equation, utilizing a different method of charting, but still retaining the moving calibrated scale. In the present paper, the true equations relating α, β, γ, and V and α, β, γ, and E are charted as nomograms of the grid type. Such graphs require for their use only a single uncalibrated straight-line index, and involve the least possible degree of visual interpolation.

Two other equations, containing only three variables, are also much used in the measurement of optic angles. These are the equations $\sin E=\beta \sin V$, and $D=K \sin E$ (Mallard's formula). The first of these was originally charted by Fedorov, using a combination of Cartesian and

* Published with the permission of the Director, U. S. Geological Survey.

polar coordinates; and subsequently Wright published two graphs of these equations, one of which was essentially a reprint of Fedorov's chart, whereas the second was a graph in Cartesian coordinates. Still later, Wright published three additional graphs of this equation, charted by the same methods. Mallard's equation, on the other hand, was first charted in Cartesian coordinates by Becke, and later in a combination of Cartesian and polar coordinates by de Souza-Brandão. A special slide-rule was also constructed for its solution by Schwarzmann. Doubtless many others have likewise prepared graphs of these two simple equations. But excepting Schwarzmann's slide-rule, which is not readily available, all of these solutions require visual interpolation whereas a three-variable nomogram is free from this drawback. None of these graphs, therefore, can be used as easily and quickly as a nomogram.

The equation $\sin E=\beta \sin V$ can readily be transformed, by a suitable choice of parameters, into Mallard's formula, and vice versa. Hence both equations convey essentially the same information, and it would be entirely feasible to chart them in a single three-line nomogram, using double calibrations on two of the scales. For the sake of clarity, however, the two equations have been separately charted.

Optic Angle Equations

Six equations are commonly given, relating the four variables α, β, γ, and V, but it is necessary to consider only two of these, both of which can be presented together in a single nomogram. The selected equations are as follows:

$$\sin^2 V_\gamma=\frac{\frac{1}{\alpha^2}-\frac{1}{\beta^2}}{\frac{1}{\alpha^2}-\frac{1}{\gamma^2}} \tag{1}$$

$$\sin^2 V_\alpha=\frac{\frac{1}{\beta^2}-\frac{1}{\gamma^2}}{\frac{1}{\alpha^2}-\frac{1}{\gamma^2}} \tag{2}$$

where V_γ = one half the true optic angle of a positive biaxial mineral.
V_α = one half the true optic angle of a negative biaxial mineral.
α = the least index of refraction.
β = the intermediate index of refraction.
γ = the greatest index of refraction.

We have also the following equations:

$$\sin E=\beta \sin V \tag{3}$$

an

$$D=K \sin E \tag{4}$$

where E = one half the apparent optic angle of a biaxial mineral, as measured in air.

D = a distance measured on a micrometer scale, usually in the lower focal plane of the ocular.

K = Mallard's constant, as experimentally determined.

Combinbing equations (1) with (3), and (2) with (3), we obtain the following equations, that are likewise to be charted:

$$\frac{\sin^2 E_\gamma}{\beta^2}=\frac{\dfrac{1}{\alpha^2}-\dfrac{1}{\beta^2}}{\dfrac{1}{\alpha^2}-\dfrac{1}{\gamma^2}} \tag{5}$$

$$\frac{\sin^2 E_\alpha}{\beta^2}=\frac{\dfrac{1}{\beta^2}-\dfrac{1}{\gamma^2}}{\dfrac{1}{\alpha^2}-\dfrac{1}{\gamma^2}} \tag{6}$$

Eliminating E from equations (3) and (4), another very useful equation is obtained, namely,

$$D=K\beta \sin V \tag{7}$$

Combining equations (1) with (7), and (2) with (7), still another useful pair of equations are made available, as follows:

$$\sin^2 V_\gamma=\frac{D^2\gamma^2}{K^2\alpha^2\gamma^2+D^2(\gamma^2-\alpha^2)} \tag{8}$$

$$\sin^2 V_\alpha=\frac{D^2\alpha^2}{K^2\alpha^2\gamma^2-D^2(\gamma^2-\alpha^2)} \tag{9}$$

For reasons later stated, nomograms of formulae (7), (8) and (9) have not been prepared

Preparation of Charts

In equation (1), let $\sin^2 V_\gamma$ be temporarily a constant, that is, let $\sin^2 V_\gamma = C$. We then have

$$(1-C).\frac{1}{\alpha^2}+C.\frac{1}{\gamma^2}-\frac{1}{\beta^2}=0$$

It is now desired to introduce into the above equation the scale moduli of the nomogram, and also to write the equation in the form of a vanishing determinant. As the values of α and γ may be nearly equal in some biaxial minerals, the range of these two variables, and also of β, may be taken as identical, and their scale moduli may be represented by the same constant, M. The transformation to a vanishing determinant is accomplished by writing two auxiliary equations in new variables, in such a manner as to produce three equations with common roots. The coefficients of these three equations will then yield the desired determinant.

Thus let $x=M.\frac{1}{\alpha^2}$, and $y=M.\frac{1}{\gamma^2}$

This change in variables yields the following equations:

$$\frac{1-C}{M}.x+\frac{C}{M}.y-\frac{1}{\beta^2}=0$$

$$x+0y-M.\frac{1}{\alpha^2}=0$$

$$0x+y-M.\frac{1}{\gamma^2}=0$$

The resulting determinant is as follows:

$$\begin{vmatrix} \frac{1-C}{M} & \frac{C}{M} & -\frac{1}{\beta^2} \\ 1 & 0 & -M.\frac{1}{\alpha^2} \\ 0 & 1 & -M.\frac{1}{\gamma^2} \end{vmatrix}=0$$

Now the index line of a nomogram must connect certain values of α, β, and γ on three scales, in such a manner as to satisfy the equations of these three variables. In other words, three points on each of the three graduated scales must lie on a straight line; and for this condition to exist, all the elements of one row or one column of a vanishing determinant must equal unity. The above determinant is readily changed into this form, by the usual methods of transformation, giving the following:

$$\begin{vmatrix} 0 & M.\frac{1}{\alpha^2} & 1 \\ C & M.\frac{1}{\beta^2} & 1 \\ 1 & M.\frac{1}{\gamma^2} & 1 \end{vmatrix}=0$$

The dimensions of the chart will be taken as S inches square, and since this chart is plotted by means of rectangular coordinates, the maximum X dimension equals S. We introduce S into the vanishing determinant merely by multiplying it into each element of the first column. The maximum Y dimension is determined by the relationship: $M=\frac{S}{\frac{1}{n_2^2}-\frac{1}{n_1^2}}$, where

where n_1 and n_2 are respectively the least and greatest value of the indices of refraction, as shown in the chart. The final constructional determinant is then as follows:

where E = one half the apparent optic angle of a biaxial mineral, as measured in air.

D = a distance measured on a micrometer scale, usually in the lower focal plane of the ocular.

K = Mallard's constant, as experimentally determined.

Combinbing equations (1) with (3), and (2) with (3), we obtain the following equations, that are likewise to be charted:

$$\frac{\sin^2 E_\gamma}{\beta^2}=\frac{\dfrac{1}{\alpha^2}-\dfrac{1}{\beta^2}}{\dfrac{1}{\alpha^2}-\dfrac{1}{\gamma^2}} \tag{5}$$

$$\frac{\sin^2 E_\alpha}{\beta^2}=\frac{\dfrac{1}{\beta^2}-\dfrac{1}{\gamma^2}}{\dfrac{1}{\alpha^2}-\dfrac{1}{\gamma^2}} \tag{6}$$

Eliminating E from equations (3) and (4), another very useful equation is obtained, namely,

$$D=K\beta \sin V \tag{7}$$

Combining equations (1) with (7), and (2) with (7), still another useful pair of equations are made available, as follows:

$$\sin^2 V_\gamma=\frac{D^2\gamma^2}{K^2\alpha^2\gamma^2+D^2(\gamma^2-\alpha^2)} \tag{8}$$

$$\sin^2 V_\alpha=\frac{D^2\alpha^2}{K^2\alpha^2\gamma^2-D^2(\gamma^2-\alpha^2)} \tag{9}$$

For reasons later stated, nomograms of formulae (7), (8) and (9) have not been prepared

Preparation of Charts

In equation (1), let $\sin^2 V_\gamma$ be temporarily a constant, that is, let $\sin^2 V_\gamma=C$. We then have

$$(1-C)\,.\frac{1}{\alpha^2}+C\,.\frac{1}{\gamma^2}-\frac{1}{\beta^2}=0$$

It is now desired to introduce into the above equation the scale moduli of the nomogram, and also to write the equation in the form of a vanishing determinant. As the values of α and γ may be nearly equal in some biaxial minerals, the range of these two variables, and also of β, may be taken as identical, and their scale moduli may be represented by the same constant, M. The transformation to a vanishing determinant is accomplished by writing two auxiliary equations in new variables, in such a manner as to produce three equations with common roots. The coefficients of these three equations will then yield the desired determinant.

Thus let $x=M.\frac{1}{\alpha^2}$, and $y=M.\frac{1}{\gamma^2}$

This change in variables yields the following equations:

$$\frac{1-C}{M}.x+\frac{C}{M}.y-\frac{1}{\beta^2}=0$$

$$x+\ 0y-M.\frac{1}{\alpha^2}=0$$

$$0x+\ y-M.\frac{1}{\gamma^2}=0$$

The resulting determinant is as follows:

$$\begin{vmatrix} \frac{1-C}{M} & \frac{C}{M} & -\frac{1}{\beta^2} \\ 1 & 0 & -M.\frac{1}{\alpha^2} \\ 0 & 1 & -M.\frac{1}{\gamma^2} \end{vmatrix}=0$$

Now the index line of a nomogram must connect certain values of α, β, and γ on three scales, in such a manner as to satisfy the equations of these three variables. In other words, three points on each of the three graduated scales must lie on a straight line; and for this condition to exist, all the elements of one row or one column of a vanishing determinant must equal unity. The above determinant is readily changed into this form, by the usual methods of transformation, giving the following:

$$\begin{vmatrix} 0 & M.\frac{1}{\alpha^2} & 1 \\ C & M.\frac{1}{\beta^2} & 1 \\ 1 & M.\frac{1}{\gamma^2} & 1 \end{vmatrix}=0$$

The dimensions of the chart will be taken as S inches square, and since this chart is plotted by means of rectangular coordinates, the maximum X dimension equals S. We introduce S into the vanishing determinant merely by multiplying it into each element of the first column. The maximum Y dimension is determined by the relationship: $M=\frac{S}{\frac{1}{n_2^2}-\frac{1}{n_1^2}}$, where

where n_1 and n_2 are respectively the least and greatest value of the indices of refraction, as shown in the chart. The final constructional determinant is then as follows:

$$\begin{vmatrix} 0 & M.\frac{1}{\alpha^2} & 1 \\ SC & M.\frac{1}{\beta^2} & 1 \\ S & M.\frac{1}{\gamma^2} & 1 \end{vmatrix} = 0 \qquad (10)$$

Similarly, by starting originally with equation (2), the following constructional determinant is obtained:

$$\begin{vmatrix} 0 & M.\frac{1}{\alpha^2} & 1 \\ S(1-C) & M.\frac{1}{\beta^2} & 1 \\ S & M.\frac{1}{\gamma^2} & 1 \end{vmatrix} = 0 \qquad (11)$$

In charting determinants (10), and (11), the question arises as to what limits should be taken for the three indices of refraction, α, β, and γ. To include all the biaxial minerals listed in the Larsen-Berman tables, the α scale should begin at 1.324, to include avogadrite; and the γ scale should extend to 4.046, to include stibnite. Limits of this magnitude are impracticable in a chart of this sort, because it is desired to plot most of the index scales with intervals of .002; and any such range would render this degree of subdivision unreadable, when the chart is reduced to its size of publication. The range of 1.450 to 2.000, which includes nearly 90 per cent of the listed minerals, was finally selected as the best possible compromise. This range excludes fewer minerals of low index of refraction than of high index of refraction, because the optical constants of the former are more readily obtained with ordinary petrographic equipment.

This chart, shown in Plate I, was drawn originally 20 inches square, for reduction to 10 inches square as a laboratory chart, and to about 7 inches square for publication. Hence $S=20$. The value of M was taken as

$$M=\frac{S}{\frac{1}{n_2^2}-\frac{1}{n_1^2}}=\frac{20}{.47562-.25}=88.645$$

The same dimensions and scale moduli were also used in the preparation of Plate II, showing the relations existing between the variables α, β, γ, and E.

In the above exposition, the value of $\sin^2 V_\gamma$ has been assumed to remain constant, representing some fixed value of V. This results in a nomogram of three graduated scales. But if a series of values are now assigned to V, the scale of $\frac{1}{\alpha^2}$ and $\frac{1}{\gamma^2}$ will remain unchanged, and a series

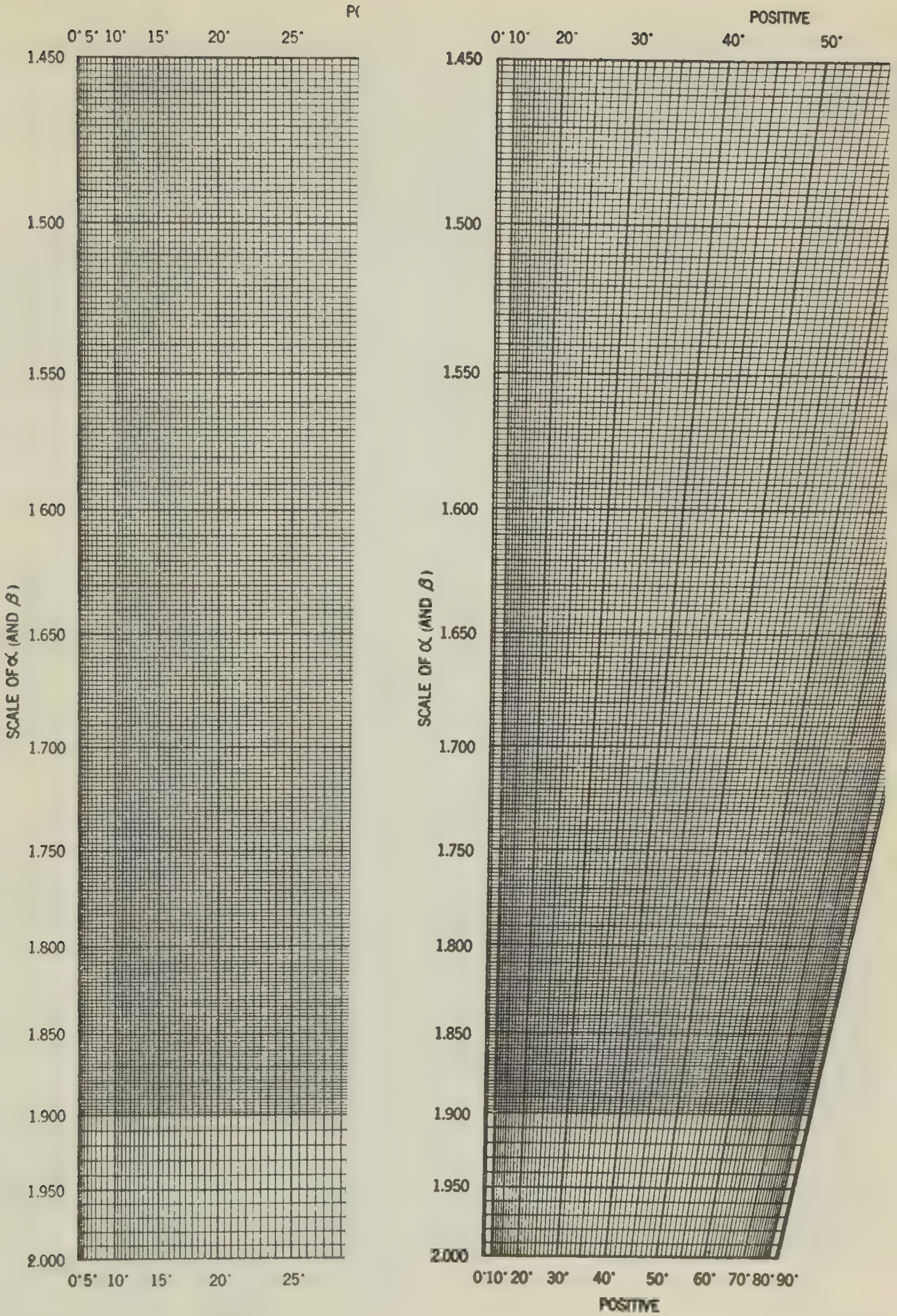
0° 5° 10° 15° 20° 25°
1.450
1.500
1.550
1 600
1.650
1.700
1.750
1.800
1.850
1.900
1.950
2.000
SCALE OF α (AND β)
0° 5° 10° 15° 20° 25°
POSITIVE
0° 10° 20° 30° 40° 50°
1.450
1.500
1.550
1.600
1.650
1.700
1.750
1.800
1.850
1.900
1.950
2.000
SCALE OF α (AND β)
0° 10° 20° 30° 40° 50° 60° 70° 80° 90°
POSITIVE

PLATE II.

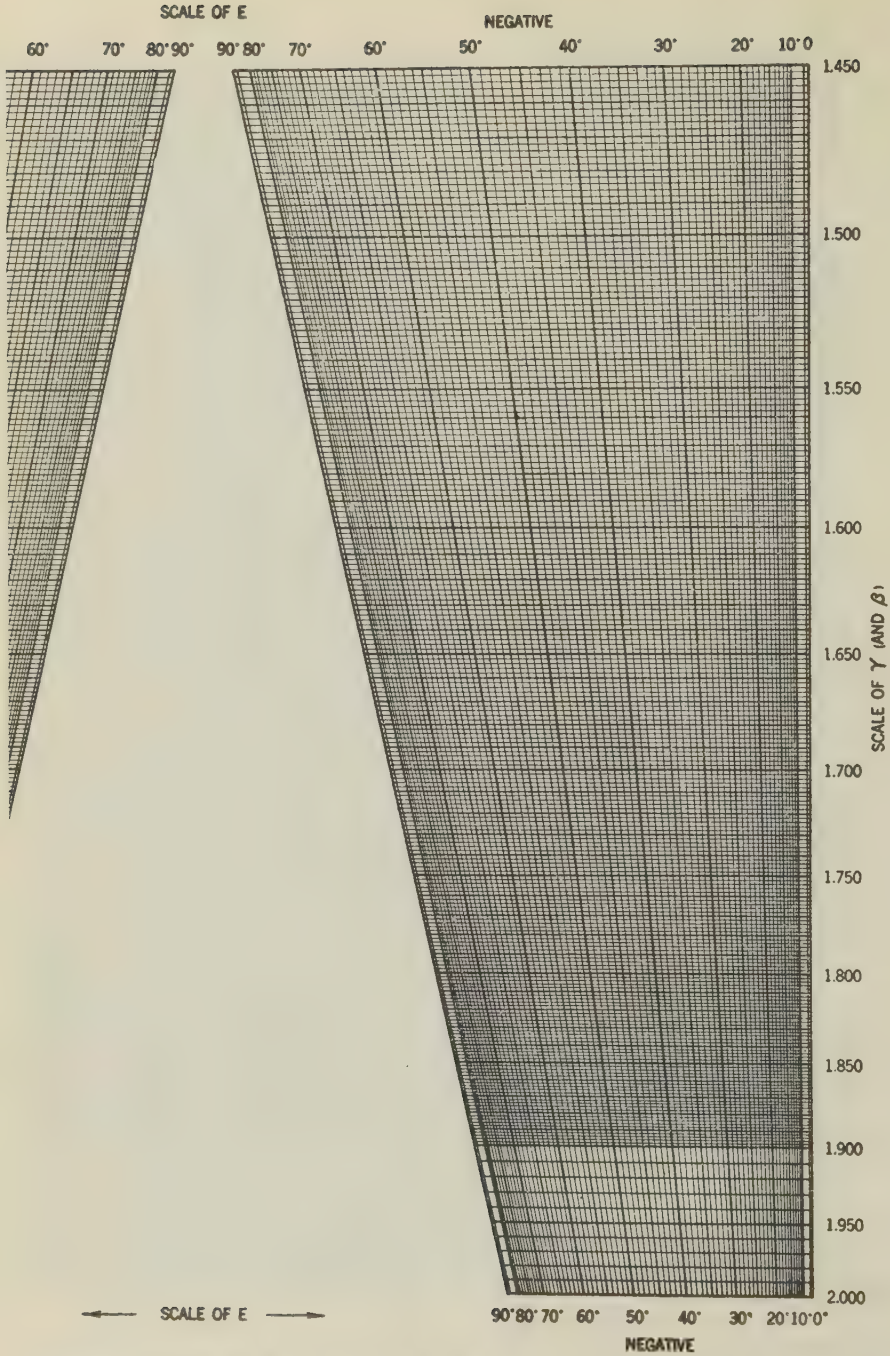

NOMOGRAM OF $\frac{\sin^2 E_\gamma}{\beta^2} = \frac{\frac{1}{\alpha^2} - \frac{1}{\beta^2}}{\frac{1}{\alpha^2} - \frac{1}{\gamma^2}}$ AND $\frac{\sin^2 E_\alpha}{\beta^2} = \frac{\frac{1}{\beta^2} - \frac{1}{\gamma^2}}{\frac{1}{\alpha^2} - \frac{1}{\gamma^2}}$

JOHN B. MERTIE, JR.
U. S. GEOLOGICAL SURVEY

of $\frac{1}{\beta^2}$ scales will be produced, each corresponding to some particular value of V. By connecting like values of $\frac{1}{\beta^2}$ on each of these scales, there will result the grid type of nomogram shown in Plate I. Charting the range of V from 0° to 45°, however, this nomogram will be confined to half the space of S inches; and in the other half it is possible to chart determinant (11) without interference. Plate I is therefore a composite grid nomogram, charting determinants (10) and (11).

Considering now equation (5), and representing $\sin^2 E_\gamma$ as temporarily a constant, we have:

$$(\beta^2-C).\frac{1}{\alpha^2}+C.\frac{1}{\gamma^2}-1=0$$

Setting $x=M.\frac{1}{\alpha^2}$ and $y=M.\frac{1}{\gamma^2}$, and utilizing the same algebraic technique already explained, we obtain the following vanishing determinant:

$$\begin{vmatrix} \frac{\beta^2-C}{M} & \frac{C}{M} & -1 \\ 1 & 0 & -M.\frac{1}{\alpha^2} \\ 0 & 1 & -M.\frac{1}{\beta^2} \end{vmatrix} =0$$

And from this, by transformation and by the introduction of S, is obtained the constructional determinant that is to be charted:

$$\begin{vmatrix} 0 & M.\frac{1}{\alpha^2} & 1 \\ SC.\frac{1}{\beta^2} & M.\frac{1}{\beta^2} & 1 \\ S & M.\frac{1}{\gamma^2} & 1 \end{vmatrix} =0 \qquad (12)$$

Similarly, by starting initially with equation (6), instead of (5), the following constructional determinant is obtained:

$$\begin{vmatrix} 0 & M.\frac{1}{\alpha^2} & 1 \\ S\left(1-C.\frac{1}{\beta^2}\right) & M.\frac{1}{\beta^2} & 1 \\ S & M.\frac{1}{\gamma^2} & 1 \end{vmatrix} \qquad (13)$$

For obvious reasons it is necessary to take for E a range of values twice as great as for V. It has been found feasible to extend the range of E from 0° to 90°, and still to chart determinants (12) and (13) in a single graph, without interference. A composite grid nomogram of this type is shown in Plate II.

In the two preceding charts (Plates I and II), the relationships are shown between α, β, γ, and V, and between α, β, γ, and E. It would also be possible to prepare a third chart, in which β, is absent, and α, γ, V and E are related. The formulae comprising this group of variables are as follows:

$$\frac{1}{\alpha^2}.\cos^2 V_\gamma+\frac{1}{\gamma^2}.\sin^2 V_\gamma=\frac{\sin^2 V_\gamma}{\sin^2 E_\gamma} \tag{14}$$

$$\frac{1}{\alpha^2}.\sin^2 V_\alpha+\frac{1}{\gamma^2}.\cos^2 V_\alpha=\frac{\sin^2 V_\alpha}{\sin^2 E_\alpha} \tag{15}$$

and the constructional determinants corresponding thereto are:

$$\begin{vmatrix} 0 & M.\dfrac{1}{\alpha^2} & 1 \\ S\sin^2 V_\gamma & M.\dfrac{\sin^2 V_\gamma}{\sin^2 E_\gamma} & 1 \\ S & M.\dfrac{1}{\gamma^2} & 1 \end{vmatrix} = 0 \tag{16}$$

$$\begin{vmatrix} S & M.\dfrac{1}{\alpha^2} & 1 \\ S\sin^2 V_\alpha & M.\dfrac{\sin^2 V_\alpha}{\sin^2 E_\alpha} & 1 \\ 0 & M.\dfrac{1}{\gamma^2} & 1 \end{vmatrix} = 0 \tag{17}$$

From a preliminary charting of these two determinants, it appears that the values of V and E will be represented by a closely spaced gridwork of two systems of lines, that intersect one another at very oblique angles. It is not believed that such a chart would be sufficiently useful to pay for the labor required in its preparation.

Consider now the charting of the next equation:

$$\sin E=\beta\sin V \tag{3}$$

Let $x=M\sin E$, and $y=N\sin V$

Substituting as before, we get the three following equations:

$$\frac{1}{M}.x-\frac{\beta}{N}.y=0$$

$$x-M\sin E=0$$

$$y-N\sin V=0$$

And from these, the following vanishing determinant is derived:

$$\begin{vmatrix} \dfrac{1}{M} & -\dfrac{\beta}{N} & 0 \\ 1 & 0 & -M\sin E \\ 0 & 1 & -N\sin V \end{vmatrix} = 0$$

This can be transformed, with S and the scale moduli M and N inserted, into the following constructional determinant:

$$\begin{vmatrix} 0 & M\sin E & 1 \\ \dfrac{SM\beta}{M\beta+N} & 0 & 1 \\ S & -N\sin V & 1 \end{vmatrix} = 0 \qquad (18)$$

In this graph, the range of E is twice that of V, and for this reason, with $M=20$, we have

$$N=\frac{S}{\sin V_2-\sin V_1}=\frac{20}{.707}=28.284$$

PLATE III. NOMOGRAM OF SIN E = β SIN V

JOHN B MERTIE JR.
U S GEOLOGICAL SURVEY

Plotting the values of X and Y in rectangular Cartesian coordinates, a chart would result having the form of a rhomboid. To obviate this, and to produce a square chart, the values of X and Y are plotted in oblique Cartesian coordinates, wherein the positive end of the Y axis makes an angle of 45° with the positive end of the X axis. Hence for a chart of 20 inches square, $S=\sqrt{800}=28.284$.

The circumstances which limited the plottable range of indices of refraction, in Plates I and II, do not apply here. Hence a more complete scale of β is charted. Equation (18) is shown in Plate III.

Using the same method as heretofore applied, equation (4) (Mallard's formula) can be transformed into the following constructional determinant:

$$\begin{vmatrix} 0 & M \sin E & 1 \\ \dfrac{SM}{NK+M} & 0 & 1 \\ S & -ND & 1 \end{vmatrix} = 0 \qquad (19)$$

In plotting determinant (19), the limits to be taken for the variables D and K are somewhat uncertain. In many petrographic microscopes, the micrometer scale used for axial angle determinations has 100 divisions, though in the Wright model Bausch and Lomb research microscope, the scale includes 130 divisions of 0.1 mm. each. Nevertheless, only a part of this scale is used, and therefore the limits of 0–50, for the half-scale of D, appear to be satisfactory. The range of K (Mallard's constant) was arbitrarily taken as twice that of D, that is, from 0 to 100. In a chart 20 inches square, the value of M is obviously 20; but $N=\dfrac{20}{50}=0.4$. The value of S, using oblique coordinates for plotting, remains 28.284. The nomogram of Mallard's formula is shown in Plate IV.

Reference has already been made to the following equations:

$$D=K\beta \sin V \qquad (7)$$

$$\sin^2 V_\gamma=\frac{D^2\gamma^2}{K^2\alpha^2\gamma^2+D^2(\gamma^2-\alpha^2)} \qquad (8)$$

$$\sin^2 V_\alpha=\frac{D^2\alpha^2}{K^2\alpha^2\gamma^3-D^2(\gamma^2-\alpha^2)} \qquad (9)$$

For all values of K, a grid nomogram would be needed to represent equation (7); and still more complex nomograms would be required to represent equations (8) and (9). On the other hand, for some fixed value of K, equation (7) could be represented by a three-line chart, and equations (8) and (9) by grid nomograms. It seems a waste of time and labor to prepare charts for all values of K, when only one, or at most a few, such

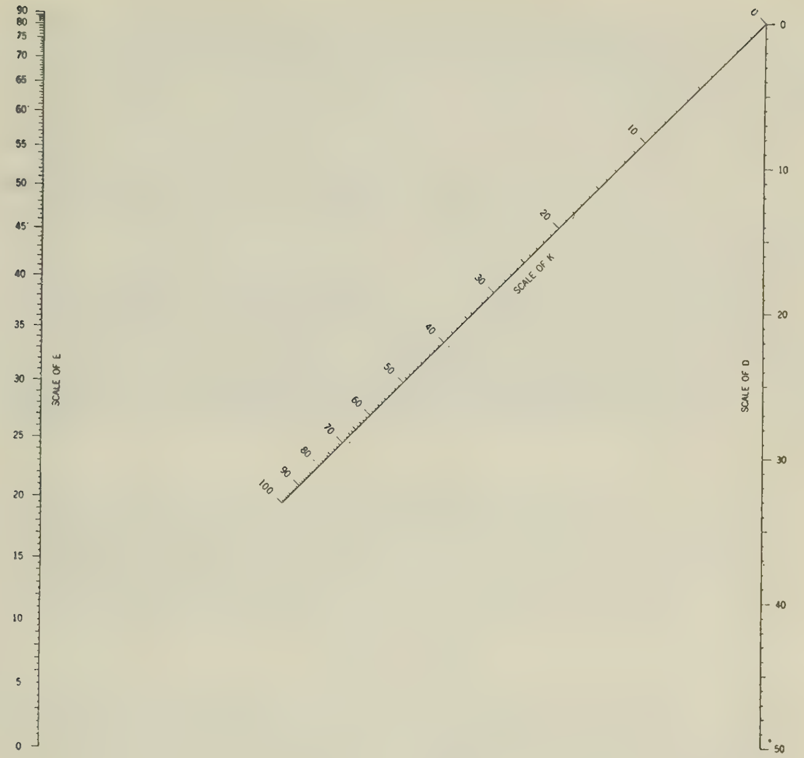

PLATE IV NOMOGRAM OF D·K SIN E (Mallard's formula)

JOHN B MERTIE, JR
U. S. GEOLOGICAL SURVEY

values are utilized by any one worker. Hence the preparation of suitable nomograms of these three formulae seems rather to be a project for the individual worker.

Use of Charts

Plates I and II merely represent graphically the relationships that exist between certain functions of α, β, γ, and V (or E); and their use is very simple. All that is really required is a straight-edge, but in actual practice it is better to use a piece of transparent celluloid or zylonite, on the bottom of which has been scratched a straight line. If this line is adjusted on the outer scales, to connect known values of α and γ, it will cut the intervening gridwork at a series of points representing specific values of β and V (or E) that satisfy the charted equations. If the value of β is known, the corresponding value of V (or E) may at once be read from the chart, and vice versa. The optical character of the mineral is likewise indicated. More generally, the value of any one variable can be found, if the values of the other three are known.

Plate I will be used mainly for computing the optic angle of a mineral from its three indices of refraction. But in actual practice, β is more difficult to determine than α and γ. Therefore, Plate II will be of value in determining the value of β, when α, γ, and E are known. The concurrent use of both charts should serve to facilitate the publication of values of α, β, γ, V and E, that accord with one another; and a critical examination of the data that have already been published, will demonstrate the need for this correlation.

Plates III and IV are ordinary N-charts that require little or no explanation. Plate III will probably be used mainly to calculate the value of V, when E and β are known. Plate IV is designed primarily for determining E, from a scale value (D) and Mallard's constant (K). In general, each of these charts shows the relationships existing between three variables.

Errors

It remains to be considered whether these charts yield solutions that have the required degree of accuracy, when considered in terms of unavoidable errors of observation. In this connection, consider formula (1).

$$\sin^2 V_\gamma = \frac{\dfrac{1}{\alpha^2}-\dfrac{1}{\beta^2}}{\dfrac{1}{\alpha^2}-\dfrac{1}{\gamma^2}}. \tag{1}$$

Differentiating partially with respect to α, β, and γ, we get:

$$\frac{\partial V_\gamma}{\partial \alpha} = -\frac{1}{\alpha^3\left(\dfrac{1}{\alpha^2}-\dfrac{1}{\gamma^2}\right)} \text{ ctn } V_\gamma$$

$$\frac{\partial V_\gamma}{\partial \beta} = \frac{1}{\beta^3\left(\dfrac{1}{\alpha^2}-\dfrac{1}{\gamma^2}\right)} \text{ cosec } V_\gamma \sec V_\gamma$$

$$\frac{\partial V_\gamma}{\partial \gamma} = -\frac{1}{\gamma^3\left(\dfrac{1}{\alpha^2}-\dfrac{1}{\gamma^2}\right)} \tan V_\gamma$$

$$\therefore dV_\gamma = \frac{1}{\dfrac{1}{\alpha^2}-\dfrac{1}{\gamma^2}}\left[-\frac{1}{\alpha^3} \text{ ctn } V_\gamma\, d\alpha + \frac{1}{\beta^3} \text{ cosec } V_\gamma \sec V_\gamma\, d\beta - \frac{1}{\gamma^3} \tan V_\gamma d\gamma\right] \tag{20}$$

Similarly from equation (2), we obtain:

$$dV_\alpha = \frac{1}{\dfrac{1}{\alpha^2}-\dfrac{1}{\gamma^2}}\left[\frac{1}{\alpha^3} \tan V_\alpha\, d\alpha - \frac{1}{\beta^3} \text{ cosec } V_\alpha \sec V_\alpha\, d\beta + \frac{1}{\gamma^3} \text{ ctn } V_\alpha\, d\gamma\right] \tag{21}$$

Now consider the mineral hornblende, for which $\alpha=1.654$, $\beta=1.666$, $\gamma=1.670$, and V (computed) $=29°49'$. The maximum error will occur when $\Delta\alpha$ and $\Delta\gamma$ are positive and $\Delta\beta$ is negative, or vice versa. Therefore we take $d\alpha=d\gamma=.001$ and $d\beta=-.001$. We then have $\frac{dV_\alpha}{V_\alpha}=.277=28$ per cent, which is approximately the maximum possible error in V. From an examination of formula (21), or by reference to Plate I, it is apparent that this error increases as the birefringence decreases. If such errors as these are present when V is numerically computed, then certainly the graphic computation of V, by the use of Plate I, is adequate.

Formulae (5) and (6) may be used either to obtain the value of E, when α, β, and γ are known; or to obtain the value of β, when α, γ and E are known. The total differentials of E_γ and E_α, for the first case, are as follows:

$$dE_\gamma=\frac{\sec E_\gamma}{\frac{1}{\alpha^2}-\frac{1}{\gamma^2}}\left[-\frac{1}{\alpha^3}\operatorname{cosec} E_\gamma(\beta^2-\sin^2 E_\gamma)d_\alpha+\frac{\beta}{\alpha^2}\operatorname{cosec} E_\gamma d\beta-\frac{1}{\gamma^3}\sin E_\gamma d\gamma\right] \quad (22)$$

$$dE_\alpha=\frac{\sec E_\alpha}{\frac{1}{\alpha^2}-\frac{1}{\gamma^2}}\left[\frac{1}{\alpha^3}\sin E_\alpha d\alpha-\frac{\beta}{\gamma^2}\operatorname{cosec} E_\alpha d\beta+\frac{1}{\gamma^3}\operatorname{cosec} E_\alpha(\beta^2-\sin^2 E_\alpha)d\gamma\right] \quad (23)$$

For the mineral hornblende, take $\alpha=1.654$, $\beta=1.666$, $\gamma=1.670$ and E_α (computed) $=55°56'$. And assume as before observational errors of $\Delta\alpha=\Delta\gamma=.001$ and $\Delta\beta=-.001$. Then $\frac{dE_\alpha}{E_\alpha}=.379=38$ per cent, which is approximately the maximum possible error in E_α. This is still greater than the maximum error that results from the numerical computation of V; and is far greater than the error that results in the graphic computation of E from Plate II.

For the other use of formulae (5) and (6), in solving for β, when α, γ, and E are known, the total differentials are as follows:

$$d\beta=\frac{1}{\beta}\left[\frac{1}{\alpha}(\beta^2-\sin^2 E_\gamma)d\alpha+\frac{\alpha^2}{\gamma^3}\sin^2 E_\gamma d\gamma+\left(1-\frac{\alpha^2}{\gamma^2}\right)\sin E_\gamma\cos E_\gamma dE_\gamma\right] \quad (24)$$

$$d\beta=\frac{1}{\beta}\left[\frac{\gamma^2}{\alpha^3}(\sin^2 E_\alpha)d\alpha+\frac{1}{\gamma}(\beta^2-\sin^2 E_\alpha)d\gamma-\left(\frac{\gamma^2}{\alpha^2}-1\right)\sin E_\alpha\cos E_\alpha dE_\alpha\right] \quad (25)$$

For hornblende, take $\alpha=1.654$, $\gamma=1.670$, $E_\alpha=60.5°$ and β (computed) $=1.6656$. The maximum error will obtain when $\Delta\alpha$ and $\Delta\gamma$ are positive, and ΔE_α is negative or vice versa. Therefore we take $d\alpha=d\gamma=.001$ and $dE_\alpha=-0.5°$. We then have $\frac{d\beta}{\beta}=.00099=.1$ per cent, which is approxi-

mately the maximum possible error in β. This error is of the order of that which results from reading β directly from the chart. It therefore appears that chart II should be satisfactory for most minerals.

The total differential of V with regard to β and E, as derived from equation (3), is as follows:

$$dV = \frac{1}{\beta}\left[\frac{\cos E}{\cos V} dE - \tan V d\beta\right] \tag{26}$$

For the mineral hornblende, assume $\beta = 1.666$, $E = 60.5°$ and V (computed) $= 31°29'$. The maximum error occurs when E and β have opposite signs. Hence taking $dE = 0.5°$ and $d\beta = -.001$, we find that $\frac{dV}{V} =$ six per cent. In Chart III, the minimum calibration of β is .02 and the minimum value to be obtained by interpolation is .01. Yet even with such readings of β, the value of V can be read closer than 6 per cent.

For reference, there are also given two other total differentials, derived from formula (4), (Mallard's formula), and formula (7). These are respectively as follows:

$$dE = \frac{1}{K}[\sec E dD - \tan E dK] \tag{27}$$

$$dV = \frac{1}{K\beta}[\sec V dD - \beta \tan V dK - K \tan V d\beta] \tag{28}$$

The total differentials above derived also lead to the consideration of another topic. Is it desirable, for example, to tabulate a value of V that is computed from α, β and γ, when the possible error in V may be as great as 28 per cent, as shown for hornblende? If the errors of observation are admitted to be as great as those assumed above, then, in the absence of other data, a more appropriate tabulation might be, $2V = 60° \pm 16°$. The same considerations apply to the tabulation of V, as computed from equation (7), because there are initial errors in β, D and K. And if E is measured directly, by the use of a Fedorov stage, it is no more free of error than any other physical measurement; and E still has to be converted to V by means of formula (3), wherein one of the variables is β, which is admittedly subject to an observational error.

In view of these considerations, it may be desirable for the mineralogist or petrographer to determine, and possibly to publish, the probable errors of observation in the basic quantities, such as α, β, γ, D and K. Estimates of these primary errors could readily be made. Thereafter these initial errors could be inserted in the total differentials above given, to compute the approximate errors that may exist in the derived quantities, such as E and V. Or if desired, the possible errors in the derived quanti-

ties could be determined by substituting in the original formulae quantities like $\alpha+\Delta\alpha$, to replace α, where the increment in the independent variable represents the probable error in that variable. It is believed that tabulations of E and V would be more useful if their possible errors were thus indicated.

References

Wright, Fred Eugene, The methods of petrographic-microscopic research, plate 9. Washington, D. C. (**1911**).

Wright, Fred Eugene, Graphical methods in microscopical petrography: *Am. Jour. Sci.*, **36,** plates 5–7 (1913).

Smith, Harold T. U., Simplified graphic method of determining approximate axial angle from refractive indices of biaxial minerals: *Am. Jour. Sci.*, **22,** 675–681 (1937).

Lane, J. H., Jr., and Smith, H. T. U., Graphic method of determining optic sign and true axial angle from refractive indices of biaxial minerals: *Am. Jour. Sci.*, **23,** 457–460 (1938).

von Fedorov, E., Universalmethode und Feldspathstudien: *Zeits. Kryst.*, **26,** heft 3, plate IV, p. 260 (1896).

Wright, Fred Eugene, *Opus cit.*, 1911 and 1913.

Becke, F., Klein'sche Lupe mit Mikrometer: *Tschermak's mineral. und petro. Mitt.*, **14,** heft 4, p. 377, (1904).

de Souza-Brandão, V., O novo microscopio da comissão do serviço geologico: *Communicações da comissão do serviço geologico de Portugal*, Tom. **5,** fasc. 1, 197–199, and plate 1 (1903).

Schwarzmann, Max., Hilfsmittel, um die Ausrechnung der Mallard'schen Formel zu ersparen: *Neues Jahrb. Mineral., Geol. und Pal.*, Jahrgang 1896, **1,** plate II, 52-56 (1896).

Larsen, Esper S., and Berman, Harry, The Microscopic Determination of the Nonopaque Minerals, second edition: *U. S. Geol. Survey, Bull.* **848,** 95–213 (1934).

BOULANGERITE

CHARLES PALACHE AND HARRY BERMAN,
*Harvard University, Cambridge, Mass.**

ABSTRACT

Boulangerite, a lead sulfantimonide, has been studied on new material, the first which has proved suitable for detailed crystallographic examination. It is monoclinic, prismatic, $2/m$, pseudo-orthorhombic. Elements $a:b:c=0.9158:1:0.3456$; $\beta=100°39\frac{1}{2}'$. Some 60 crystal forms were observed. Lattice constants (Berry): $a_0=21.14$ Å, $b_0=23.46$ Å, $c_0=8.07$ Å, $\beta=100°48'$. New analyses by Gonyer on Washington boulangerite confirmed Shannon's earlier analysis and Berry's cell content of $Pb_{40}Sb_{32}S_{88}$.

CRYSTALLOGRAPHY

Boulangerite is one of the many fibrous sulfantimonides of lead concerning the crystal form of which little of a definite nature has hitherto been known. Its slender striated prisms generally show no terminal faces. Sjögren (1897) measured crystals from Sala, Sweden, which he regarded as orthorhombic, and on the basis of a single domal face he was able to establish an axial ratio. Shannon (1921) found a single pyramid face on a crystal from Stevens County, Washington, and also inferred orthorhombic symmetry but obtained an axial ratio in very poor agreement with that of Sjögren.

New studies on boulangerite from three localities have been successful in revealing its true crystallographic nature. The mineral proves to be monoclinic with an astonishing wealth of forms. The results of these studies are presented in the following pages.

The first measurable crystals of boulangerite were found in small vugs of a massive, coarsely fibrous material from Rocker Gulch Placer Claim near Deerlodge, Montana (Specimen No. 92671). This material was supplied by Ward's Natural Science Establishment and bore the name geocronite. In addition to the dominant boulangerite, there is coarsely granular sphalerite present, crytsals of pyrite, and, in a single cavity, crystals of bournonite, identified by crystal measurement, and showing the forms:—

c 001	*e* 210	Σ 031	*z* 201	*p* 223	*O* 213
a 100	*κ* 013	*x* 102	*φ* 113	*y* 111	*v* 211
m 110	*n* 011	*o* 101	*u* 112	*g* 221	

The boulangerite crystals are needles of dark iron-gray color, less than a half millimeter in diameter and from a few to ten or more millimeters

* Contribution from the Department of Mineralogy and Petrography, Harvard University, No. 253.

in length. Since they project from the walls of vugs, they are all singly terminated. The needles are very brittle, the slightest pressure causing them to break into thin leaf-like flakes along a single pinacoidal cleavage, which proved to be parallel to $a\{100\}$. The prisms are deeply striated parallel to their length so that they gave generally a continuous chain of weak or colored signals on the goniometer, but the best crystals gave a consistent series of prism forms. The numerous terminal faces are so minute and so irregular as to give under the binoculars no definite clue of symmetrical distribution; but their weak signals gave position angles which when projected yielded a definite pattern, repeated, although with great variation in the forms present, on successive crystals. By plotting the measurements of each crystal on transparent paper and superimposing these projections, with rotation about the projection center, parallelism was obtained and the form series was developed.

The projection showed apparent orthorhombic symmetry as regards spacing of poles. However, the radial zones to prism faces did not intersect in the projection center but rather at a point about ten degrees off center—a point not represented by a crystal face on any of the crystals at first measured. This fixed the symmetry as probably monoclinic, a conclusion strengthened by each succeeding measurement and subsequently proved by x-ray study as reported on a later page.

Identical crystallographic characters including the wealth of forms were later found on boulangerite from the Gold Hunter Mine, Mullan, Idaho, described by Shannon (1918) as "mullanite"; and on crystals from Stevens County, Washington, also analyzed by Shannon (1925).

Boulangerite is, then, monoclinic but with pronounced pseudosymmetry both orthorhombic and tetragonal, as shown in the gnomonic projection, Fig. 1, which presents several unusual features. Although there is an unusually rich form series, one primary zone [010], parallel to the symmetry plane, is almost missing since both $\{100\}$ and $\{001\}$ are seldom found and only one orthodome, $\{101\}$, is at all common. The axial zone [001] is of course strong, the crystals being strongly prismatic in that direction and showing four well-established prism forms. The clinodome zone [100] is also well marked. A strange feature of this projection is the absence of poles in the central area. $\{001\}$, $\{011\}$ and $\{\bar{2}01\}$ are among the rarest forms and the unit pyramid $\{111\}$ has been found on but two crystals. If these be omitted, there are but three forms which have a slope angle (ρ) less than 40°.

The lattice of boulangerite is pseudo-orthorhombic because x_0' is almost exactly half of p_0', another case like that of brochantite recently described by Palache (1939). It is pseudotetragonal because p_0' and q_0' are so nearly equal and the ϕ of $\{110\}$ is about 48°.

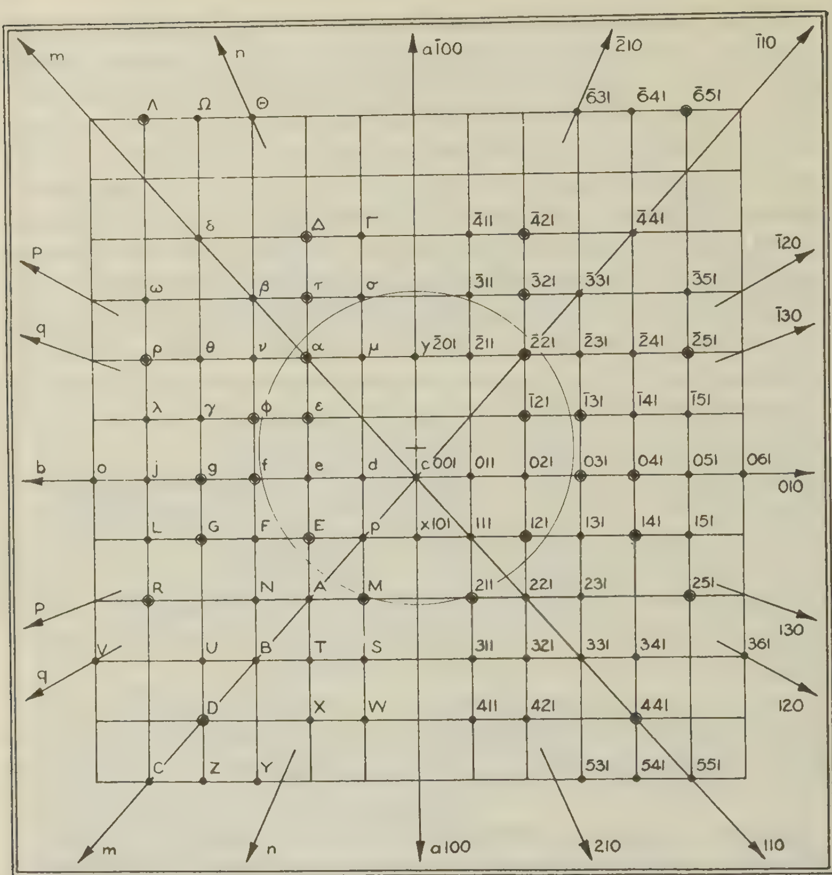

FIG. 1. Gnomonic projection of boulangerite. ⊙ indicates most common forms.

The combinations of forms found on eight crystals from Montana, five from Idaho, and two from Washington are shown in Table 1. From this table it appears that the most frequently occurring forms on Montana crystals are: a, q, m, n, f, g, D, δ, G, ϕ, R, ρ, X, and Λ; on Idaho crystals c, m, f, x, α, E, and ϕ; on Washington crystals f, x, A, α, G, ϕ, and θ. Of these forms only two, $f\{031\}$ and $\phi\{\bar{1}31\}$ are among the commonest for all three localities. Several, however, are common on two localities. It is clear that many forms occur at all the localities and that a larger number are confined to one. This last fact may be due to the better and more numerous crystals measured from Montana. At least ten forms not listed were found once only on the Montana crystals.

Table 1. Combinations of Forms on Boulangerite

Locality	Montana								Idaho					Washington	
Crystal	1	2	3	4	5	6	7	8	1	2	3	4	5	1	2
c 001										x		x	x		
b 010	x	x		x		x									
a 100	x	x	x			x	x		x						
q 130	x		x	x	x		x								
P 120										x					
m 110	x	x	x	x	x	x	x	x	x	x	x			x	
n 210		x	x	x	x	x	x	x	x	x				x	
d 011										x		x			
e 021								x	x					x	
f 031	x		x	x	x			x	x	x	x			x	x
g 041			x	x	x		x	x							
j 051		x		x	x			x							
o 061	x							x							
x 101							x	x	x			x	x	x	x
y $\bar{2}01$												x	x	x	
p 111										x					
A 221			x				x				x			x	x
B 331	x		x	x	x										
D 441	x			x	x		x	x							
C 551		x				x									x
α $\bar{2}21$								x	x	x	x	x	x	x	x
β $\bar{3}31$		x		x			x	x							
δ $\bar{4}41$		x		x	x		x	x							
E 121								x	x	x	x	x		x	
F 131			x		x			x							
G 141	x	x	x	x	x	x	x	x						x	x
L 151						x									
ϵ $\bar{1}21$								x		x	x				
ϕ $\bar{1}31$		x		x	x			x	x	x	x			x	x
γ $\bar{1}41$		x						x							
λ $\bar{1}51$				x	x										
M 211								x	x		x				
N 231			x	x	x		x								
R 251	x	x		x	x	x		x							
μ $\bar{2}11$								x		x				x	
ν $\bar{2}31$				x				x							
θ $\bar{2}41$			x	x			x	x						x	x
ρ $\bar{2}51$	x		x	x	x			x							
S 311		x					x	x							
T 321	x	x	x												x

TABLE 1—*Continued*

Locality	Montana								Idaho					Washington	
Crystal	1	2	3	4	5	6	7	8	1	2	3	4	5	1	2
U 341	x	x			x	x									
V 361				x	x			x							
σ $\bar{3}11$				x			x	x					x		
τ $\bar{3}21$								x	x		x				
ω $\bar{3}51$		x			x			x							
W 411	x						x	x							
X 421	x		x	x	x			x							
Γ $\bar{4}11$				x			x								
Δ $\bar{4}21$				x			x	x							
Y 531	x	x				x									
X 541		x												x	
Θ $\bar{6}31$				x			x								
Ω $\bar{6}41$				x	x			x						x	
Λ $\bar{6}51$		x		x	x			x	x						

TABLE 2*a*. MEASURED ANGLES ON BOULANGERITE FROM MONTANA

		No.	Meas. Aver.		Range		Calculated	
			ϕ	ρ	ϕ	ρ	ϕ	ρ
b	010	4	0°27′	90°00′	−2°38′–+2°35′	—	0°00′	90°00′
a	100	5	88 44	90 00	89 04 – 94 48	—	90 00	90 00
q	130	6	20 20	90 00	19 39 – 21 09	—	20 19½	90 00
m	110	22	47 55½	90 00	47 15 – 48 42	—	48 01	90 00
n	210	18	65 39	90 00	65 00 – 66 15	—	65 46½	90 00
e	021	1	15 14	35 53	—	—	15 14	35 37
f	031	5	10 25	46 34½	9 21 – 10 55	46°25′–46°43′	10 17½	46 30
g	041	6	7 58	54 09½	7 31 – 8 27	54 14 –55 00	7 45	54 22
j	051	5	6 13	60 06	5 59 – 6 31	59 49 –60 30	6 13	60 05½
o	061	2	5 07½	64 21	4 46 – 5 29	64 18 –64 24	5 11	64 20½
x	101	2	90 04½	29 52	89 28 – 90 41	29 50 –29 54	90 00	29 46½
A	221	2	53 39½	50 25	52 58 – 54 21	49 45 –57 05	54 08½	49 43
B	331	5	52 18	59 25	52 02 – 52 26	59 17 –59 34	52 16½	59 27
D	441	6	51 18	65 39	51 05 – 51 27	65 32 –65 55	51 16½	65 39
C	551	2	50 08	70 01½	49 50 – 50 26	70 00 –70 03	50 39½	69 51½
α	$\bar{2}21$	1	−39 37	41 56	—	—	−39 59½	42 03½
β	$\bar{3}31$	5	−42 37½	55 00	42 12 – 42 52	54 40 –55 22	−42 54½	54 45½
δ	$\bar{4}41$	5	−44 21	62 59	43 34 – 45 52	62 40 –63 30	−44 16½	62 37

TABLE 2a—*Continued*

		No.	Meas. Aver.		Range		Calculated	
			ϕ	ρ	ϕ	ρ	ϕ	ρ
E	121	1	39 43	42 10	—	—	39 37	41 54
F	131	3	29 09	49 51	29 05 – 29 11	49 22 –50 20	28 53½	49 49½
G	141	10	22 29	56 16	21 16 – 23 16	56 00 –57 04	22 29	56 14½
L	151	1	18 14	61 16	—	—	18 19½	61 13
ϵ	$\bar{1}21$	1	−15 19	35 45	—	—	−15 49	35 41½
ϕ	$\bar{1}31$	5	−10 52	46 08	10 09 – 11 23	45 34 –46 33	−10 41½	46 32
γ	$\bar{1}41$	2	− 8 20	54 37½	8 11 – 8 28	54 30 –54 45	− 8 03½	54 23½
λ	$\bar{1}51$	3	− 6 02	59 57	5 39 – 6 29	59 47 –60 05	− 6 28	60 06
M	211	1	69 41	45 37	—	—	70 07½	45 28½
N	231	4	42 30	54 40	41 43 – 42 51	54 25 –55 00	42 41	54 40
R	251	8	29 06	63 14½	28 42 – 29 30	63 00 –63 37	28 57½	63 08½
μ	$\bar{2}11$	1	−59 53	33 15	—	—	−59 12	34 01
ν	$\bar{2}31$	3	−27 50	50 03	27 01 – 28 46	49 38 –50 30	−29 13	49 54½
ϕ	$\bar{2}41$	5	−22 35½	56 26	22 19 – 23 04	56 09 –56 45	−22 45	56 17½
ρ	$\bar{2}51$	6	−18 32½	61 14	18 10 – 19 05	60 55 –61 33	−18 33	61 15
S	311	3	75 30	54 25	75 12 – 75 44	54 20 –54 32	75 32½	54 09
T	321	3	62 45	56 30	62 41 – 62 50	56 16 –56 54	62 43	56 27
U	341	5	44 05	62 28	43 45 – 44 20	62 00 –62 52	44 06½	62 33
V	361	3	32 54	67 58	32 49 – 33 00	67 12 –68 35	32 52½	67 57
σ	$\bar{3}11$	4	−69 55½	45 28	−69 31 – 70 10	45 19 –45 33	−70 16½	45 40½
τ	$\bar{3}21$	2	−54 10	49 46	−54 09 – 54 11	49 43 –49 49	−54 21	49 52
ω	$\bar{3}51$	3	−28 56	63 29	−28 43 – 29 08	63 12 –64 00	−29 09	63 11½
W	411	3	79 09	60 19	78 25 – 80 01	60 00 –60 42	78 40	60 22½
X	421	8	68 17	61 33	67 49 – 68 39	61 16 –61 50	68 09½	61 42½
Γ	$\bar{4}11$	2	−75 35	54 31	−75 32 – 75 38	54 22 –54 40	−75 37	54 17½
Δ	$\bar{4}21$	4	−62 35	56 25	−62 13 – 63 09	56 12 –56 32	−62 51	56 34
Y	531	5	64 00	66 50	−63 26 – 64 42	66 36 –67 12	63 48½	66 56½
Z	541	1	56 25	68 13	—	—	56 45	68 22
Θ	$\bar{6}31$	3	−63 46	67 04	−63 40 – 63 53	66 53 –67 20	−63 53½	67 00
Ω	$\bar{6}41$	3	−56 36	68 21	−56 19 – 56 47	68 15 –68 27	−56 50½	68 25
Λ	$\bar{6}51$	4	−50 28	70 00½	−50 10 – 50 41	69 45 –70 18	−50 45½	69 53½

Table 2b. Measurements on Boulangerite from Idaho.

		No.	Meas. aver.		Range		Calculated	
			ϕ	ρ	ϕ	ρ	ϕ	ρ
c	001	3	88°58′	12°01′	88°58′–90°00′	10°42′–13°20′	90°00′	10°39½′
a	100	1	88 40	90 00	—	—	90 00	90 00
P	120	2	29 05	90 00	28 24 –29 46	—	29 03½	90 00
m	110	8	48 23	90 00	47 41 –49 03	—	48 01	90 00
n	210	3	66 11	90 00	65 03 –67 00	—	65 46½	90 00
d	011	3	29 37	21 25	28 20 –30 48	21 13 –21 40	28 34½	21 29
e	021	1	16 27	41 42	—	—	15 14	35 47
f	031	6	10 33	46 32	9 44 –11 29	46 06 –46 54	10 17½	46 30
x	101	3	90 24	29 46	90 00 –91 00	29 37 –29 53	90 00	29 46½
y	$\bar{2}01$	2	−90 23	30 05	90 23 –90 23	—	−90 00	30 06½
p	111	1	60 44	33 37	—	—	58 52	33 45½
A	221	1	54 14	49 14	—	—	54 08½	49 43
α	$\bar{2}21$	5	−39 57	41 32	−38 36 –41 23	41 23 –42 10	−39 59½	42 03½
E	121	5	39 56	41 39	39 42 –40 14	41 06 –42 00	39 37	41 54
ϵ	$\bar{1}21$	4	−15 22	35 38	−15 03 –16 00	35 34 –35 55	−15 49	35 41½
ϕ	$\bar{1}31$	4	−10 38	46 02	−10 15 –11 19	45 08 –46 00	−10 41½	46 32
M	211	2	69 43	45 48	69 21 –70 05	45 30 –46 06	70 07½	45 28½
μ	$\bar{2}11$	1	−56 14	34 48	—	—	−59 12	34 01
σ	$\bar{3}11$	1	−69 12	45 10	—	—	−70 16½	45 40½
τ	$\bar{3}21$	3	−54 19	49 34	53 31 –55 06	49 10– 49 52	−54 21	49 52
Λ	$\bar{6}51$	1	−51 17	69 50	—	—	−50 45½	69 53½

Table 3. Angle Table. Boulangerite

Monoclinic, prismatic $\dfrac{2}{m}$

$a:b:c = 0.9158:1:0.3456;\ \beta = 100°39\tfrac{1}{2}'$
$p_0:q_0:r_0 = 0.3774:0.3396:1;\ \mu = 79°20\tfrac{1}{2}'$
$r_2:p_2:q_2 = 2.9443:1.1111:1;\ p_0' = 0.3840 \quad q_0' = 0.3456 \quad x_0' = 0.1882$

Forms		ϕ	ρ	ϕ_2	$\rho_2 = B$	C	A
c	001	90°00′	10°39½′	79°20½′	90 00′	—	79°20½′
b	010	0 00	90 00	—	0 00	90°00′	90°00′
a	100	90 00	90 00	0 00	90 00	79 20½	—
***r*	140	15 31½	90 00	0 00	15 31½	87 52	74 28½
**q*	130	20 19½	90 00	0 00	20 19½	86 19	69 40½
**P*	120	29 03½	90 00	0 00	29 03½	84 51	60 56½

TABLE 3—*Continued*

Forms		ϕ	ρ	ϕ_2	$\rho_2 = B$	C	A
**m*	110	48 01	90 00	0 00	48 01	82 06	41 59
**n*	210	65 46½	90 00	0 00	65 46½	80 17½	24 13½
***l*	310	73 18	90 00	0 00	73 18	79 48	16 42
***k*	410	77 19	90 00	0 00	77 19	79 36½	12 41
***i*	510	79 48	90 00	0 00	79 48	79 30½	10 12
***h*	710	82 40½	90 00	0 00	82 40½	79 26	7 19½
d	011	28 34½	21 29	79 20½	71 14½	18 45½	79 55
e	021	15 14	35 37	79 20½	55 48½	34 11½	81 12
f	031	10 17½	46 30	79 20½	44 28	45 32	82 33½
g	041	7 45	54 22	79 20½	36 21½	53 38½	83 42½
j	051	6 13	60 05½	79 20½	30 29½	59 30½	84 37
o	061	5 11	64 20½	79 20½	26 08½	63 51½	85 19½
***u*	102	90 00	20 49	69 11	90 00	10 09½	69 11
x	101	90 00	29 46½	60 13½	90 00	19 07	60 13½
y	$\bar{2}01$	−90 00	30 06½	120 06½	90 00	40 46	120 06½
p	111	58 52	33 45½	60 13½	73 18	25 10½	61 35½
A	221	54 08½	49 43	46 17	63 27½	41 26	51 48½
B	331	52 16½	59 27	36 43½	58 12	51 17	47 04
D	441	51 16½	65 39	30 07	55 15½	57 33	44 42
C	551	50 39½	69 51½	25 22½	53 28½	61 47	43 26½
α	$\bar{2}21$	−39 59½	42 03½	120 06½	59 07½	49 27	115 30
β	$\bar{3}31$	−42 54½	54 45½	133 56½	53 15½	62 20½	123 47
δ	$\bar{4}41$	−44 16½	62 37	143 25½	50 31½	70 17	128 18½
E	121	39 37	41 54	60 13½	59 02½	35 53	64 47½
F	131	28 53½	49 49½	60 13½	48 01	45 23	68 20
G	141	22 29	56 14½	60 13½	39 48½	52 46½	71 27½
L	151	18 19½	61 13	60 13½	33 41½	58 23½	74 00½
ϵ	$\bar{1}21$	−15 49	35 41½	101 04½	55 51	39 45½	99 09
ϕ	$\bar{1}31$	−10 41½	46 32	101 04½	44 30	49 22½	97 44½
γ	$\bar{1}41$	− 8 03½	54 23½	101 04½	36 23½	56 53	96 33
λ	$\bar{1}51$	− 6 28	60 06	101 04½	30 31½	61 51	95 36
M	211	70 07½	45 28½	46 17	75 58½	36 03	47 53½
N	231	42 41	54 40	46 17	53 09	47 52½	56 25½
R	251	28 57½	63 08½	46 17	38 41	58 24½	64 24½
μ	$\bar{2}11$	−59 12	34 01	120 06½	73 21½	43 28½	118 43½
ν	$\bar{2}31$	−29 13	49 54½	120 06½	48 06½	55 40½	111 55½

TABLE 3—*Continued*

Forms		ϕ	ρ	ϕ_2	$\rho_2 = B$	C	A
θ	$\bar{2}41$	−22 45	56 17½	120 06½	39 54	60 56	108 46
ρ	$\bar{2}51$	−18 33	61 15	120 06½	33 47	65 05½	106 11½
S	311	75 32½	54 09	36 43½	78 49½	43 53	38 17½
T	321	62 43	56 27	36 43½	67 32½	47 09	42 12½
U	341	44 06½	62 33	36 43½	50 25	55 26½	51 51
V	361	32 52½	67 57	36 43½	38 53	62 29	59 47½
σ	$\bar{3}11$	−70 16½	45 40½	133 56½	76 01½	55 48	132 20
τ	$\bar{3}21$	−54 21	49 52	133 56½	63 32½	58 46	128 24½
ω	$\bar{3}51$	−29 09	63 11½	133 56½	38 47½	68 43½	115 46
W	411	78 40	60 22½	30 07	80 10	49 57	31 32
X	421	68 09½	61 42½	30 07	70 52½	51 54	35 11
Γ	$\bar{4}11$	−75 37	54 17½	143 25½	68 22	64 39½	141 52
Δ	$\bar{4}21$	−62 51	56 34	143 25½	67 37	66 10	137 57
Y	531	63 48½	66 56½	25 22½	66 02½	57 29	34 20½
Z	541	56 45	68 22	25 22½	59 21½	59 35½	38 59
Θ	$\bar{6}31$	−63 53½	67 00	154 42	66 06½	76 38½	145 45
Ω	$\bar{6}41$	−56 50½	68 25	154 42	59 25½	77 26	141 07
Λ	$\bar{6}51$	−50 45½	69 53½	154 42	53 33½	78 16	136 39½

* Forms also found by Sjögren.
** Forms found only by Sjögren.

Since the crystals are all so minute that the faces are practically invisible even under the binoculars, it was not deemed advisable to attempt to figure them, as drawings would only be conventional representations at best. Crystal eight from Montana with faces of 33 forms is by far the most complex one seen.

For the reason given in the last paragraph no attempt has been made here to characterize the individual forms and their relative importance must be judged solely by frequency of occurrence.

Table 2*a* contains a summary of the angular measurements obtained from the eight Montana crystals and Table 2*b* similar figures for those from Idaho. The Washington crystals were of far inferior quality and are not recorded. If there appears to be a somewhat wide range in the observed angles of individual forms, it must be remembered that all of these measurements were obtained from crystal facets so minute that often the signal was but the faintest spot of light. It was impossible to distinguish the faces on most of the crystals sufficiently clearly to recognize their symmetry relations. Only after projection could the orientation of the crystal be determined, and it was a matter of astonishment to find

how closely these weak reflections repeated on each new projection the pattern of the common gnomonic lattice. The Montana crystals gave, on the whole, the better reflections, but both sets of measurements were used to calculate elements with the following concordant results:

Boulangerite, Montana	$a:b:c=0.9158:1:0.3456$; $\beta=100°39\frac{1}{2}'$
Boulangerite, Idaho	$a:b:c=0.9252:1:0.3437$; $\beta=100°52'$

The first set of elements, based on measurements of 90 faces of 17 forms on 8 crystals, was accepted as best established and was used in the calculation of an angle table, Table 3.

Reference has been made earlier to the paper in which Sjögren first described crystals of boulangerite. His results have been correlated with our established position by the following transformation formula and they show excellent correspondence.

Transformation, Sjögren to Palache 041/800/002
Elements of Sjögren, calculated to new position: $a:b:c=0.9315:1:0.3383$; $\beta=100°27\frac{1}{2}'$

Four of his prisms were found on our crystals. Five others, probably very weak forms, were not found by us but are included in the angle table as well as his single terminal form, which becomes the dome {102}.

The measurements of Shannon (1921) could not be satisfactorily correlated with our position.

X-Ray Crystallography

Dr. Hurlbut reports as follows on his study of x-ray photographs made in 1939 on crystals of boulangerite from Montana. From measurements of a rotation photograph: $d_{001}=8.00$ Å. From Weissenberg zero and second-layer photographs: $d_{010}=23.16$ Å and $d_{100}=21.10$ Å. $\mu=79°19'$ calculated from x-ray data. Hence, $a_0=21.47$, $b_0=23.16$, $c_0=8.00$.

$a_0:b_0:c_0=0.9166:1:0.3475$; $\beta=100°41'$ compared with
$a:b:c=0.9158:1:0.3456$; $\beta=100°39\frac{1}{2}'$

Space group $P2_1/a$ fixed by the conditions
hkl all present
$0k0$ present only with k even
$h00$ present only with h even
$h0l$ present only with h even

This cell taken with the measured specific gravity, 5.98, gives $M_0=14468$.

These results agree very closely with the measurements published by Berry (1940), which were made on boulangerite from Mullan Co., Idaho, the so-called mullanite for which the crystal measurements are given above.

Chemical Composition

Boulangerite from Rocky Gulch, Montana, was analyzed by Gonyer on a carefully selected sample prepared by Dr. Berman. The density was determined on the microbalance as 5.98 ± 0.02, the mean of many measurements by several observers. Gonyer also analyzed the Stevens Co., Washington, boulangerite and confirmed Shannon's analysis. This second analysis is interpreted in the following table prepared by Dr. Berman.

Table 4. Analysis of Boulangerite from Washington

	1	2	3	4	5
Pb	55.42	55.28	55.91	39.03	40
Sb	25.69	25.40	25.69	30.53	32
S	18.89	18.19	18.40	83.03	88
Fe		.39			
Insol.		.62			
Total	100.00	99.88	100.00		

1. $Pb_5Sb_4S_{11}$.
2. Boulangerite from Cleveland Mine, Stevens Co., Washington, U.S.N.M. 95414. *Pb* and *S* average of two determinations. F. A. Gonyer, analyst.
3. Column 2 recalculated to 100%.
4. Atoms per unit cell with $M_0 = 14468$ and $d = 5.98$.
5. $8(Pb_5Sb_4S_{11})$.

The experience of Mr. Gonyer in making this analysis proved that the complete separation of lead and antimony was not attained by some well-tried methods, leading to low results for lead. This observation suggests that possibly the numerous earlier analyses of boulangerite with low lead content may have been at fault through this determinative error. For instance, the so-called plumosite of English writers with a formula given as $Pb_2Sb_2S_5$ has physical characteristics differing in no way from boulangerite

References

Berry, L. G., *Univ. of Toronto Studies, Geol. Series* No. **44,** 5 (1940).
Palache, C., *Am. Mineral.*, **24,** 463 (1939).
Shannon, L. V., *Am. Jour. Sci.*, **45,** 66 (1918).
———, *Am. Jour. Sci.*, **1,** 423 (1921).
———, *Jour. Wash. Acad. Sci.*, **15,** 195 (1925).
Sjögren, H., *Geol. För. Förh.*, **19,** 153 (1897).

INESITE, $Mn_7Ca_2Si_{10}O_{28}(OH)_2 \cdot 5H_2O$*

W. E. RICHMOND,
Geological Survey, U. S. Department of the Interior, Washington, D. C.

ABSTRACT

A new orientation of inesite has been chosen with the elements: $a:b:c=0.9700:1:1.3208$; $\alpha=87°42'$, $\beta=132°35\frac{1}{2}'$, $\gamma=97°01'$ (Sheibe's elements transformed by the formula $\bar{1}0\bar{1}/0\bar{1}0/001$). X-ray measurements on a cleavage fragment gave $a_0=8.89$, $b_0=9.14$, $c_0=12.14$; $a_0:b_0:c_0=0.973:1:1.328$; $\alpha=87°38\frac{1}{2}'$, $\beta=132°30'$, $\gamma=97°05\frac{1}{2}'$. This orientation has been selected to make the direction of elongation the c-axis and to retain the similarity inesite shows to members of the wollastonite group. Inesite is shown to be closely related to a high calcium rhodonite which theoretically may be considered as a dehydrated inesite. From published analyses and a new specific gravity determination, together with the lattice constants, the cell formula is calculated to be $Mn_7Ca_2Si_{10}O_{28}(OH)_2.5H_2O$.

INTRODUCTION

The chemical and optical data of inesite have been summarized and a new occurrence at Quinault, Washington, has been described by Miss J. J. Glass and W. T. Schaller.[1] They showed that neither of the two simple formulae generally given for inesite, with a 1:1 ratio of $RO:SiO_2$, are compatible with the analyses, and that MnO and CaO do not vary reciprocally. They were unable, however, to determine a simple formula for the mineral and proposed the complex one $15SiO_2 \cdot 3CaO \cdot 11MnO \cdot 10H_2O$. On the basis of x-ray studies, the more probable and simpler formula is $10SiO_2 \cdot 2CaO \cdot 7MnO \cdot 6H_2O$. This closely approximates two-thirds of the formula proposed by Glass and Schaller. Moreover, when this simpler formula is written $Mn_7Ca_2Si_{10}O_{28}(OH)_2 \cdot 5H_2O$, the chemical relation of inesite to rhodonite can be more clearly demonstrated.

During the course of an investigation of members of the wollastonite family composed of such minerals as wollastonite, pectolite, bustamite, and rhodonite, the writer was impressed by the outward similarity of inesite to these minerals.[2] An x-ray investigation of inesite was undertaken to determine whether this similarity was fortuitous. The first results obtained did not indicate any apparent structural relation to members of the wollastonite group. However, it will be shown that a close relation does exist between inesite and rhodonite, and the writer[3] has pointed out that there is a relation between rhodonite and wollastonite. This relation " . . . is confined to near equality of two of the principal lattice periods and the included axial angle; the remaining lattice parameters are quite dissimilar." Recent work by the writer, as yet unpublished,

* Published by permission of the Director, Geological Survey, Washington, D. C.

[1] Glass, J. J., and Schaller, W. T., Inesite: *Am. Mineral.*, **24**, 26–39 (1939).

[2] The inter-relationship of these and other minerals will be shown in a forthcoming paper.

[3] Richmond, W. E., On babingtonite: *Am. Mineral.*, **22**, 640 (1937).

indicates that "the remaining lattice parameters" of rhodonite are in simple rational relationship to the corresponding parameters of wollastonite. Without entering into details, which will be fully dealt with in a forthcoming paper, wollastonite and rhodonite may be considered as belonging to separate groups within the same family. As inesite and rhodonite are structurally related, they should belong to the same group and should be included in the family containing members of the wollastonite group. This group is composed of such minerals as wollastonite, pectolite, schizolite, and bustamite.

Crystallography

The material used for the x-ray investigation was selected from the same specimen from Quinault, Washington, that was studied by Glass and Schaller. Single crystals were not found; a cleavage fragment, therefore, approximating $0.5\times 0.25\times 0.75$ mm. in size was used. The rotation axis was taken as the edge between the two perfect cleavages. This axis is the direction of greatest elongation. Rotation, zero, first, and second layer-line photographs were taken about the axis of elongation from which were calculated the six lattice parameters. The results are:

$$a_0 = 8.89\text{ Å} \quad a_0:b_0:c_0 = 0.973:1:1.328$$
$$b_0 = 9.14\text{ Å} \quad \alpha = 87°38\tfrac{1}{2}', \beta = 132°30', \gamma = 97°05\tfrac{1}{2}'$$
$$c_0 = 12.14\text{ Å}$$

The unit cell, although its orientation does not conform to the normal triclinic setting, is a simple cell and has been selected to make the elongation the direction of the c-axis. The edge between the two perfect cleavages is also the direction of the elongation; the cleavages were taken as $\{100\}$ and $\{010\}$. This orientation likewise corresponds to that of most other members of the wollastonite family, in that the two cleavages are taken as the pinacoidal forms in the prism zone in second permutation. That is, triclinic wollastonite is reoriented so that the direction of elongation (corresponding to the b-axis of monoclinic parawollastonite) is taken as the c-axis.

The orientation of the chosen unit cell does not conform to the cell based on the morphology adopted by Scheibe as given in Dana,[4] but does confrm if the cell derived from Scheibe's orientation is rotated 180° about the c-axis. The forms and elements of Scheibe are transformed to the new orientation by the matrix $\bar{1}0\bar{1}/0\bar{1}0/001$. The axial ratios and angles so obtained, namely: $a:b:c = 0.9700:1:1.3208$, $\alpha = 87°42'$, $\beta = 132° 35\tfrac{1}{2}'$, $\gamma = 97°01'$, agree closely with those obtained from the x-ray calculations. Therefore, the transformed elements of Scheibe were used in calculating the angle table (Table 1).

[4] Dana, E. S., *A System of Mineralogy*, 6th ed., 564 (1892).

Table 1. Inesite: Angle Table

Inesite—$Mn_7Ca_2Si_{10}O_{28}(OH)_2 \cdot 5H_2O$
Triclinic, pinacoidal—$\bar{1}$

$a:b:c = 0.9700:1:1.3208$; $\alpha = 87°42'$, $\beta = 132°35\frac{1}{2}'$, $\gamma = 97°01'$
$p_0:q_0:r_0 = 1.3709:0.9789:1$; $\lambda = 86°40'$, $\mu = 47°21'$, $\nu = 82°35'$
$p_0' = 1.8652$, $q_0' = 1.3330$; $x_0' = 0.9192$, $y_0' = 0.0792$

Forms		ϕ	ρ	A	B	C
c	001	85°05½′	42°41½′	47°21′	86°40′	—
b	010	0 00	90 00	82 35	—	86°40′
a	100	82 35	90 00	—	82 35	47 21
M	$1\bar{1}0$	120 33½	90 00	37 58½	120 33½	56 28½
f	201	83 04½	77 52	12 08½	83 14	35 13
e	$\bar{1}01$	−99 51½	43 21½	133 18½	96 45	85 57½
l	$\bar{2}01$	−98 14½	70 24	160 23	97 45½	113 02
g	$\bar{3}01$	−97 55	77 55½	167 55	97 44½	119 41
d	$\bar{1}11$	−38 27	56 14½	115 23	49 23	84 23½

Rare forms $\{3\bar{3}2\}$, $\{\bar{1}.0.12\}$
Doubtful forms $\{0\bar{4}7\}$, $\{3\bar{4}6\}$

Content of the Unit Cell

The analysis of inesite from Quinault given by Glass and Schaller,[5] the determined specific gravity (3.03), together with the molecular weight of the unit cell (1322.6) were used in calculating the contents of the unit cell. The results are given in Table 2.

Table 2. Inesite: Content of the Unit Cell

	1	2	3		4	5	6
SiO_2	45.67	45.42	.7562		10.01	10	45.57
MnO	35.10	34.91	.4922	6.51			37.68
FeO	0.92	0.92	.0128	0.17	6.96	7	
MgO	0.86	0.86	.0213	0.28			
CaO	9.33	9.28	.1655		2.19	2	8.53
H_2O	8.66	8.61	.4783		6.33	6	8.22
	100.54	100.00					100.00

Specific gravity: determined = 3.03. Calculated from molecular weight of the unit cell and composition = 3.02. Calculated from the specific energies and indices of refraction = 2.94.

1. Analysis of inesite from Quinault, Washington; analyst, J. G. Fairchild.
2. Recalculated to 100%.
3. Molecular proportions.
4. Number of molecules in the unit cell.
5. Theoretical number of molecules in the unit cell.
6. Calculated analysis on the basis of the formula $Mn_7Ca_2Si_{10}O_{28}(OH)_2 \cdot 5H_2O$.

[5] Glass and Schaller, *op. cit.*, p. 28.

The composition of inesite derived from column 5 is $Mn_7Ca_2Si_{10}O_{28}(OH)_2 \cdot 5H_2O$. Schaller has shown that the percentages of SiO_2, MnO, and CaO are remarkably constant in the seven listed analyses of inesite from various localities. The ratios SiO_2:MnO:CaO determined from column 4 of Table 2 closely approximate 10:7:2. The same ratios are apparent in the other listed analyses.

The formula, $Mn_7Ca_2Si_{10}O_{28}(OH)_2 \cdot 5H_2O$, after all the water has been deducted, approximates closely that of a high-calcium rhodonite. Gossner and Brückl[6] have shown that the cell content of rhodonite is $(Mn, Fe, Ca)_{10}Si_{10}O_{30}$ or $10(RSiO_3)$. This has been verified by the writer. A high-calcium rhodonite with a ratio MnO:CaO of 7:2 would have the composition $Mn_{7.78}Ca_{2.22}Si_{10}O_{30}$, shown in column 1 of Table 3. This may be compared with the composition $Mn_{6.54}Ca_{2.46}Si_{10}O_{29}$ of inesite from Quinault, after deducting total water and recalculating to 100 per cent.

Table 3. Comparison of the Composition of a High-Calcium Rhodonite with that of Inesite, Water Deducted

	Rhodonite $Mn_{7.78}Ca_{2.22}Si_{10}O_{30}$	Inesite, deducting H_2O and calculating to 100 per cent $Mn_{6.54} \cdot Ca_{2.46} \cdot Si_{10}O_{29}$
SiO_2	47.04	49.70
MnO	43.20	38.20
FeO	—	1.01
MgO	—	0.94
CaO	9.76	10.15
	100.00	100.00

A comparison of the two columns indicates that the composition of a high-calcium rhodonite and dehydrated inesite is approximately the same except that one of the manganese positions in inesite is unoccupied. The formulae for rhodonite and for a dehydrated inesite may also be written:

Rhodonite	$(Mn, Ca)_{10}Si_{10}O_{30}$
Dehydrated inesite	$(Mn, Ca)_9Si_{10}O_{29}$

If inesite is assumed to be a hydrated high-calcium rhodonite with rhodonite having a cell formula $R_{10}Si_{10}O_{30}$, then the sum of the RO group in inesite should be 10 if all the water were present as H_2O. The preponderance of evidence shows, however, that the sum of the RO

[6] Gossner, B., and Brückl, K., Über strukturelle Beziehungen von Rhodonit zu anderen Silikaten: *Centralbl. Min.*, **A**, 320 (1928).

group in inesite is 9. This requires that two hydroxyl groups replace two oxygens, leaving one cation position unoccupied. The remaining water is present as H_2O. This may be expressed as follows, considering all the R as Mn, for brevity:

Rhodonite	$Mn_{10}Si_{10}O_{30}$
Inesite	$Mn_9Si_{10}O_{28}(OH)_2$.

When 2 O^{--} is replaced by $2(OH)^-$ the excess charge in the cation position is compensated by the removal from the structure of a cation with charge 2+. This structure may be termed unsaturated. The unsaturated structure may be seen also in babingtonite with the cell formula $Ca_4Fe_2''Fe'''_2Si_{10}O_{28}(OH)_2$. The structure contains two unoccupied cation positions, owing to the presence of ferric iron as well as the replacement of oxygen by hydroxyl.

A saturated structure, one in which all cation positions are occupied, may be illustrated by pectolite [$Na_2Ca_4Si_6O_{16}(OH)_2$]. If pectolite is assumed to be wollastonite ($Ca_6Si_6O_{18}$) with an additional hydroxyl and sodium, then the sodium with a valence of one, occupies positions in the wollastonite structure formerly occupied by Ca^{++}. Thus all cation positions are occupied and the structure is saturated. This may be seen more clearly by a comparison of the two formulae

Wollastonite	$Ca_6Si_6O_{18}$
Pectolite	$Na_2Ca_4Si_6O_{16}(OH)_2$

In wollastonite the six cation positions are occupied by $6Ca^{++}$. In pectolite the six cation positions are occupied by $4Ca^{++}$ plus $2Na^+$.

The assumption has been made that inesite may be considered as a hydrated calcium rhodonite. Conversely, high-calcium rhodonite may be considered as a dehydrated inesite. In order to test this assumption a specimen of powdered (100 mesh) inesite from Quinault was dehydrated by heating for seven hours at 800° C. in a stream of nitrogen. A powder photograph was taken of this material and compared with powder photographs of unheated inesite and of rhodonite. A reproduction of these photographs is shown in Fig. 1.

The powder photograph of the heated inesite is nearly identical with that of rhodonite and is dissimilar to that of the unheated inesite. Therefore, inesite may be assumed to bear a close structural relation to rhodonite and this relation should appear in a comparison of the lattice constants.

Comparison of x-ray powder photographs shows that the picture of dehydrated inesite is much closer to that of rhodonite than to that of pyroxmangite.

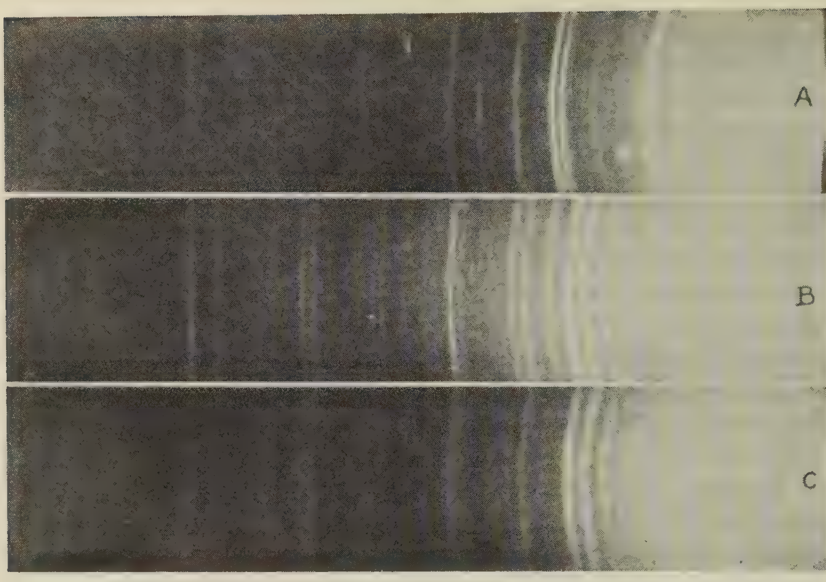

FIG. 1. Powder photographs of (A), inesite; (B), rhodonite; and (C), inesite after dehydration at 800° C.

The lattice constants of rhodonite in the orientation of inesite together with those of inesite are given below.

	Rhodonite[a]	*Inesite*
a_0	6.65	8.89
b_0	7.85	9.14
c_0	12.16	12.14
V_0*	571.37	720.41
α	91°38′	87°38½′
β	114°53½′	132°30′
γ	96°38′	97°05½′

[a] These figures are derived from x-ray data by the writer, as yet unpublished.
* = Volume of the unit cell.

If inesite is to be considered as basic hydrated rhodonite, the increase in the volume of inesite over that of rhodonite is due to the introduction of H_2O into the rhodonite lattice. A comparison of the cell edge lengths shows that this introduction has probably taken place along the b-axis in such a manner as to increase the length of c_0 (34 per cent increase) approximately twice as much as that of a_0 (16 per cent increase). This differential increase in the lengths of a_0 and c_0 is reflected in a distortion of the rhodonite lattice by a large increase in the β angle.

The dehydrated inesite which had previously been crushed to 100 mesh, when placed in immersion oils and examined under the microscope,

is seen to have undergone only a slight shrinkage. The individual fragments, when observed under low magnifications, extinguish almost as a unit. Under high magnification, the extinction is seen to be slightly undulatory, but no more so, according to W. T. Schaller,[7] than the massive rhodonite which has replaced johannsenite in specimens of these minerals from Mexico. The birefringence is low, most of the fragments showing only gray of the first order with but occasional patches of red and very occasionally small areas of blue of the second order. The birefringence does not exceed 0.015 and hence agrees with the birefringence of rhodonite (0.013) and is considerably different from the much higher birefringence of inesite (0.035).

When first placed in immersion oils, the extreme indices of the dehydrated inesite, as observed, are about 1.67 and 1.685. Miss J. J. Glass obtained an average index of about 1.68 with apparent extremes of about 1.67 and 1.69, after soaking in the index oils for three days. After immersion for several months, the average index seemed to drop about 0.01.

These values of the indices of refraction of the dehydrated inesite are much higher than the γ value of inesite (1.651), but appreciably lower than the indices of high-calcium rhodonite (with about 10 per cent of CaO) which are approximately $\alpha = 1.715$, $\beta = 1.72$, $\gamma = 1.73$.

The lower values of the indices of the dehydrated inesite as compared with those of a high-calcium rhodonite, may be a reflection of the unsaturated structure in which one cation position is unoccupied.

No satisfactory observations on the size or sign of the axial angle could be made.

In conclusion, it is well to point out that the expressed relations between rhodonite and dehydrated inesite are not to be taken as implying an actual genesis in nature of one of these minerals from the other. There is no evidence that any inesite has actually been derived from rhodonite. It is pertinent, however, to note that in the Harstig mine, Wermland, Pajsberg, Sweden, inesite occurs with rhodonite and from the same mine, another hydrated manganese aluminum silicate, ganophyllite, is reported to surround crystals of rhodonite. It is possible, however, that under proper conditions either one of the two minerals, inesite or rhodonite, may be converted to the other. Therefore, it is well to bear in mind, when examining suites of minerals containing either of these minerals, that there is a possibility of finding one of these minerals being replaced by the other.

[7] W. T. Schaller examined the dehydrated inesite under the microscope and prepared the description of his observations.

THE MINERALOGY OF METAMORPHOSED SERPENTINE AT HUMPHREYS, FRESNO COUNTY, CALIFORNIA

A. Pabst,

University of California, Berkeley, California

Abstract

Nodules of metamorphosed serpentine which were described by MacDonald[1] have been reexamined. New observations have shown that several minerals not recognized by MacDonald exist in these nodules. Their presence largely explains some of the inconsistencies of his description.

Careful examination of the succession of metamorphic zones about several nodules shows that the changes varied greatly from nodule to nodule, and even in different parts of the same nodule. It is impossible to summarize these changes in a single scheme or graph.

Introduction

Last year there appeared in this journal a discussion of "progressive metasomatism of serpentine"[1] by G. A. MacDonald in which the mineralogy of the materials considered aroused the interest of the writer. MacDonald described certain zoned nodules of serpentine in a rock which he called biotite schist. The nodules occur in a roadcut on California State Highway 168, just west of Humphreys, Fresno County, California. MacDonald has described the locality and the geologic setting at length.[2]

For a better understanding it is necessary to repeat some of the main features of MacDonald's description of the nodules. He states that they vary "in diameter from about 10 cm. to over a meter." They are spherical to flattened ellipsoidal and consist of a "core of massive grayish-green serpentine" entirely enclosed in several zones of varying composition. The thickness of these zones does not increase with the size of the nodule. The boundaries between the zones are, in part, rather sharp. *The serpentine core*[3] is essentially antigorite. It is surrounded successively by *the talc zone*, composed largely of talc with some serpentine, chlorite and "ore minerals"; *the talc-actinolite zone*, the "inner part" consists of felty talc in which lie needles of actinolite with 18° extinction angle, making up 5 per cent of the rock; "middle," similar to the inner part, but with 40 per cent actinolite; and an "outer part" consisting largely of actinolite in long blades with $\gamma = 1.646$ ($\pm .003$). The extinction angle is not men-

[1] MacDonald, G. A., Progressive metasomatism of serpentine in the Sierra Nevada of California: *Am. Mineral.*, **26**, 276–287 (1941).

[2] *Op. cit.*, and Geology of the western Sierra Nevada between the Kings and San Joaquin Rivers, California: *Univ. Calif. Publ., Bull. Dept. Geol. Sci.*, **26**, 215–286 (1941).

[3] The italics in this paragraph correspond to those of MacDonald.

tioned. Rosiwal analysis of a section shows "actinolite = 89.1 per cent, talc = 7.9, chlorite = 2.6, ore = 0.4." *The biotite zone* is "composed largely of biotite, generally with about 10 per cent of actinolite and a little chlorite."

All this may seem plausible, but MacDonald also published and discussed three analyses which furnish evidence of the misidentification of some of the more important constituents. Moreover, he drew a graph to represent the "compositions of successive zones" based on these three chemical analyses and on "two micrometric analyses." As will be shown this diagram is misleading because it omits from representation certain parts of the zones which were not properly covered by the analyses.

The Analyses

MacDonald's first analysis is of the serpentine and requires no comment. The other two contain evidence of misidentification of principal constituents.

Table 1

SiO_2	54.14	Na_2O	0.19
TiO_2	0.19	K_2O	0.08
Al_2O_3	2.52	H_2O-	0.07
Fe_2O_3	3.42	H_2O+	3.34
FeO	7.17	CO_2	none
MnO	0.22	P_2O_5	none
MgO	25.35	S	0.03
CaO	2.82	Cr_2O_3	0.28
			99.82

The second analysis (see Table 1) is of the "outer part of the radial talc-actinolite zone," for which the Rosiwal analysis is quoted above. The material is described as largely "actinolite" and MacDonald calculated the composition of this mineral, giving it only 3.2 per cent CaO. No actinolite analysis has thus far been published which showed so little lime. In 29 analyses tabulated by Doelter, the minimum CaO content is 10.50 per cent, and most of the values lie between 11 and 14 per cent. This is in excellent accord with the theoretical composition of $(OH)_2Ca_2(Mg,Fe)_5(Si_8O_{22})$ which would permit variation between 11.44 per cent CaO for the magnesian end-member, and 16.68 per cent for the ferrous end-member, the name actinolite being applied to only a portion of this range. The limits of its application need not concern us here. In any case the material analyzed lies well outside the limits and is *not* actinolite.

There are several amphiboles that are very low in calcium. The monoclinic cummingtonite series tends to be richer in ferrous iron, whereas the orthorhombic anthophyllite series is richer in magnesium. The

analysis suggests anthophyllite and this is in harmony with the optical data quoted above. Reexamination of many specimens confirms this interpretation.

Table 2

SiO_2	37.46	Na_2O	0.53
TiO_2	0.87	K_2O	0.19
Al_2O_3	14.64	H_2O-	6.89
Fe_2O_3	7.57	H_2O+	8.89
FeO	1.22	CO_2	none
MnO	0.09	P_2O_5	0.06
MgO	19.66	S	0.04
CaO	1.66	Cr_2O_3	0.07
			99.93

MacDonald's third analysis is of the "biotite rim" (see Table 2). The sample is said to contain "about 95 per cent biotite," whose optical properties were given as "small negative optic angle, $\beta=1.565$ ($\pm.003$), and X = nearly colorless to very pale yellow, Y and Z = yellowish-brown." The analysis must have seemed unusual, for he says "it shows the mineral to be a phlogopitic variety, low in iron and alkalies, especially K_2O, and fairly high in magnesia." The analysis shows only 0.19 per cent K_2O, less than one-fiftieth the amount required by the formula and far below the range, 6 to 10 per cent, common for biotite, including even the most "phlogopitic." On the other hand, MacDonald paid little attention to the high water content (total 15.78 per cent), nearly four times that required by the phlogopite formula. In this case the interpretation again is not far to seek. The biotite-like material, which must have made up most of the analyzed samples, was in all probability vermiculite. Such optical properties of this mineral as are given by MacDonald might apply equally well to vermiculite or to phlogopite. An explanation of the slightly low water content for vermiculite, and the rather high lime, will be suggested in the conclusion. Many vermiculite analyses, however, show a small CaO content and it will be fruitless to try to determine, in this particular case, just how much of it is due to contamination. The analysis as a whole suggests vermiculite and reexamination has shown that this is the chief constituent of the micaceous crust of some of the nodules.

The Reexamination

The writer was not acquainted with the locality, or the material, at the time MacDonald did his work. The reexamination was begun on a suite of specimens collected in February 1940 by Dr. Richard Merriam and Mr. A. L. Repecka, and kindly made available to the writer by the latter. One of these specimens is almost identical in size and appearance

with that shown in MacDonald's Fig. 2 *A*, which seems to have formed the basis for much of his discussion. In April 1942 the writer visited the locality. Though the exposure had suffered slightly from rain wash, the nodules were easily located and the relations could be seen very clearly. Many specimens were collected, including one very much like MacDonald's Fig. 2 *B*.

The material collected by the writer was mostly taken from the cut on the south side of state highway 168, about 140 paces west of the intersection at Humphreys. Here the nodules are embedded in a fine grained friable rock called "mica schist" by MacDonald. They can be seen at intervals in the cut for a distance of at least sixty feet. Several score of feet to the east, serpentine makes the entire walls of the cut and extends to the above mentioned intersection, whereas granitic rocks are found a few hundred feet to the west and extend westward for some distance as indicated on the map, MacDonald's Fig. 1. Small irregular patches of quartz, aplite, serpentine and granitic rock are interspersed with the "mica schist," their contacts being obscure.

MacDonald states that "the mica schist in which the zoned nodules are enclosed is composed largely of brown biotite, with a smaller amount of quartz and a little orthoclase and oligoclase." The writer collected several specimens of this rock adjoining and within a few feet of the metamorphosed serpentine nodules. A bromoform separation of the heavy minerals for the purpose of securing a sample of the biotite in this rock for comparison with the micaceous minerals of the nodules, yielded a concentrate consisting mostly of dirty green hornblende. This seemed unusual and so extra large thin sections were made from two specimens of this rock. The maximum grain dimensions do not exceed 1 mm. and the average dimensions are of the order of one or two tenths of a millimeter. The texture is granular with only a slight orientation of some of the minerals; an ideal case for micrometric analysis. The results for the two slides were:

	Plagioclase	*Hornblende*	*Biotite*	*Quartz*	*Magnetite*
I	55%	27	16	1	1
II	54	24	20	1	1

The plagioclase is mostly oligoclase. Apatite is conspicuous but was not included in the micrometric analysis. The composition is that of an igneous rock. It hardly seems proper to call it a mica schist and its mineral composition is quite different from that given by MacDonald.

It is evident from MacDonald's paper that he worked mostly with thin sections showing only fragments of the zone succession. In fact, several paragraphs of his paper begin with references to thin sections

cut from a certain zone or part of a zone. It has long been the writer's conviction that effective petrographic study requires, among other things, the use of large sections and low magnifications in order that microscopic petrography may be more than mere mineral determination. Only in this way can the relations of several minerals, the texture and structure of the assemblage and, as in the present case, the transition from one zone to another, be properly observed.

Accordingly a pair of thin sections measuring about 20 by 40 mm. each were prepared from each of six specimens. The core and the enclosing rock are not cut by these sections, but every one shows the entire succession of zones from the micaceous crust to the talc zone. The innermost shell breaks away from the core easily in many specimens and no sections show this sharp boundary between the massive gray-green antigorite and its mantle of felted white talc. The nature of the contact between the micaceous crust and the "schist" matrix cannot even be observed well in the field, or in the hand specimen, since the matrix is very friable and the micaceous crust tends to fall away from materials on either side of it. Nevertheless, all sections show at least a little of this crust.

In order to observe the complete thin sections, whose area is many times that visible under even the lowest magnification of any petrographic microscope, they were also studied between polaroid sheets and one of each pair (i.e., six sections) were photographed full size between crossed polaroids at 4 diameters. The observations thus gained, together with immersion study of all constituents in each of these and several other specimens and auxiliary experiments mentioned below, yielded a rather detailed picture of the mineralogy and succession of zones.

MacDonald recognized that the zones are not uniformly developed about all of the specimens, or even about an entire nodule. Nevertheless he emphasized and discussed at length the particular zone succession whose description is briefly given in the first part of this paper. My observations do not warrant such a procedure, but two features seem constant in all the specimens:—

A. The innermost zone is always dominantly felted talc with only minor amounts of other minerals which may include chlorite, magnetite, and monoclinic amphibole.

B. The outermost zone is always micaceous, but the character of the micaceous minerals varies.

The mineralogy and succession of the intermediate zones are highly diverse. Some samples of this diversity are recorded in Table 3 which gives the complete zone successions found in several sections.

TABLE 3. SUCCESSION OF ZONES OBSERVED IN SEVERAL SECTIONS NORMAL TO CRUST OF METAMORPHOSED SERPENTINE NODULES

I	II	III*a*	III*b*
7 mm. Chlorite	2 mm. Chlorite	1 mm. Vermiculite	4½ mm. Coarse chlorite
33 mm. Talc with some chlorite	4 mm. Tremolite partly changed to talc	3 mm. Coarse tremolite	33 mm. Felted and radial talc containing chlorite and magnetite with pressure shadows
	6 mm. Felted and radial talc	20 mm. Radial anthophyllite with some talc	
	15 mm. Radial tufty anthophyllite		
	10 mm. Talc with nests of magnetite and chlorite	8 mm. Talc with some tremolite	

The recorded thickness of the micaceous crust is in all cases less than its total thickness. MacDonald mentions 7 mm. as a maximum thickness for this zone. This may be correct for those places where it consists largely of vermiculite, but chlorite crusts locally reach a thickness of 30 mm. or more. The recorded thickness of the innermost zone is, of course, likewise less than its total, but the figures given for the intermediate zones indicate their true thickness, as all sections were cut carefully at right angles to the zone boundaries.

The zone successions recorded in Table 3 as III*a* and III*b* were observed on different parts of the same large nodule. The only correspondence in the mineralogy of the zones is in the predominance of talc in the inner part. If suitable allowances are made for the misdetermination of minerals mentioned above, III*a* corresponds roughly to the succession discussed in detail by MacDonald. Figures 1 and 2 show the greater part of each of these successions. The difference between the two amphiboles in III*a* is readily apparent.

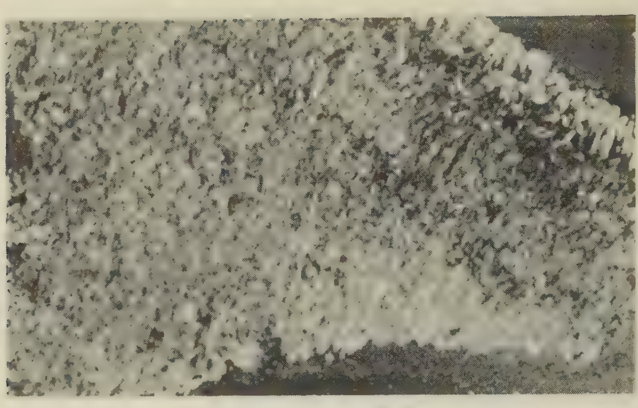

FIG. 1. Thin section normal to surface of nodule between crossed polaroids.

FIG. 2. Thin section normal to surface from another part of the same nodule shown in Fig. 1. Between crossed polaroids.

Since there is such variability in the zones it may be more satisfactory to discuss the mineralogy of the nodules, mineral by mineral rather than zone by zone.

Vermiculite. This mineral was found to constitute most of the micaceous crust of several specimens. In these specimens the crust is only a few millimeters thick. The properties of the vermiculite vary slightly and it is most easily identified by its very low specific gravity, near 2.3, which clearly distinguishes it from all other constituents. In every case where the micaceous crust is composed of vermiculite, it directly overlies a zone of tremolite and some prisms of tremolite are embedded in the vermiculite. It was also seen in streaks or nests in a specimen closely resembling MacDonald's Fig. 2 *B*. These streaks are doubtless identical with what he called "dark veinlets of biotite."

A detailed examination of the vermiculite was carried out on the specimen, collected by Merriam and Repecka, which closely resembles MacDonald's Fig. 2 *A*. The properties of this vermiculite are:—

G. (Berman balance) = 2.29
G. (suspension) = 2.27
Optically negative, moderate birefringence,
$\beta = 1.552 \pm 0.003$
$2V =$ ca. 20°, (Mallard's method)
Pleochroism:
Z and Y, yellowish brown;
X, nearly colorless
Ignition loss = 19.1%
Loss at about 650° C. = 15.1%

This leaves no doubt as to the identity of the mineral. The specific gravity is higher than the value for ideal vermiculite given by Gruner,[4] but is close to that reported by him for a vermiculite from near Pilot, Md., having nearly the same water content.

The refractive index is a little lower than that reported by MacDonald for what he called "biotite," but in other specimens it was found to vary to over 1.57, above MacDonald's value but still within the recognized range for vermiculite.[5]

The ignition loss indicates that the water content of this vermiculite is about normal. The water content of seven vermiculites studied by Gruner ranges from 17.80 to 21.4 per cent, averaging 19.7 per cent. The fact that about 4 per cent water is retained to a relatively high temperature is in harmony with Gruner's interpretation that vermiculite changes to a material of talc-like structure upon partial dehydration. This partly dehydrated material appears to have a very low density, but this is only because of its exfoliated condition. Under the microscope the material appears cloudy and its properties cannot be accurately determined, but the mean index remains in the neighborhood of 1.57.

The behavior of the vermiculite upon dehydration was studied with the aid of differential thermal curves.[6] Figures 3 shows such curves for

[4] Gruner, J. W., The structure of vermiculites and their collapse by dehydration: *Am. Mineral.*, **19**, 557–575 (1934).

[5] Shannon, E. V., Vermiculite from the Bare Hills near Baltimore, Maryland: *Am. Jour. Sci.*, **15**, 20–24 (1928).

[6] Grim, R. E., and Howland, R. A., Differential thermal analysis of clay minerals: *Am. Mineral.*, **27**, 223 (1942).

the Humphreys vermiculite and several related materials. All curves were made at a heating rate of about $9\frac{1}{4}°$ per minute and run from room temperature to about 1040° C.

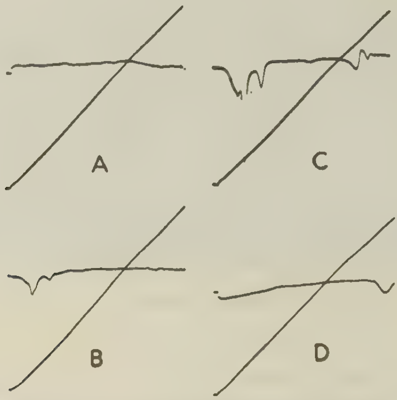

FIG. 3. Differential thermal curves. (Prepared by Dr. J. B. Page.) A. Biotite; B. Hydrobiotite; C. Vermiculite; D. Talc.

The curve for biotite (A) was made on material separated from the Half Dome quartz monzonite, Yosemite National Park. It was obtained at or near the locality where Turner[7] collected biotite for analysis. There is little doubt that this is essentially the same material. Its specific gravity was found by Berman balance to be 3.03 (Turner gave 3.05). It is nearly uniaxial and its mean refractive index is about 1.65. The water loss given in the analysis by Hillbrand is 1.03 per cent at 105° and 3.64 per cent above 105°. The curve gives no indications that there are any marked heat effects due to sudden loss. All the other curves show one or more breaks indicating water loss at a particular temperature or at a high rate over a small temperature interval.

The talc curve (D) was made on material taken from the stock of the Division of Soil Science. This talc, labelled "Providence, Rhode Island," is in large, silvery white, flakes, obviously very pure material. It is optically negative, nearly uniaxial, has a mean index of 1.582 ± 0.003, and its specific gravity is about 2.78. Its total water content (determined by Dr. J. B. Page) is 5.38 per cent. The weight loss up to 725°, determined as the differential thermal curve was being run, was only 0.85 per cent. This shows that over 4 per cent water, essential to the structure of talc, is retained to a rather high temperature. It may be that this and the other curves give slightly high values for the temperatures at which

[7] Turner, H. W., Some rock-forming biotites and amphiboles: *Am. Jour. Sci.*, (4) **7**, 294–298 (1899).

Table 4. Powder Pattern of Vermiculite Encrusting Zoned Nodules of Serpentine Near Humphreys, Fresno County, California

Observations (Pabst)		Ideal vermiculite (Gruner)			Average of observations on 6 vermiculites (Gruner) Intensity
Intensity	Spacing	Indices	Spacing	Intensity	
10	13.72	002	14.12	451	10
		004	7.06	21	0.3
		006	4.71	13	0.5
4	4.583	020	4.60	55	1
3	3.545	008	3.530	137	3.5
2+	2.86	0010	2.824	106	4
		130	2.650	25	
		$20\bar{2}$	2.650	13	
		$13\bar{2}$	2.635	39	
4 b	2.65	200	2.634	18	1
		132	2.576	102	
		$20\bar{4}$	2.575	53	
		$13\bar{4}$	2.534	302	
6 b	2.55	202	2.533	151	1.5
		134	2.432	28	
		$20\bar{6}$	2.431	13	
8	2.393	$13\bar{6}$	2.374	454	3.5
		204	2.373	219	
		0012	2.353	13	
1	2.264	136	2.250	27	
		$20\bar{8}$	2.249	14	
2	2.187	$13\bar{8}$	2.186	214	1
		206	2.186	103	
2	2.078	138	2.058	92	1
		$20\overline{10}$	2.058	48	
2	2.030	0014	2.017	104	1
		$13\overline{10}$	1.996	57	1
		208	1.995	29	
		1310	1.875	19	
		$20\overline{12}$	1.875	11	
1	1.836	$13\overline{12}$	1.817	103	1
		2010	1.817	54	
		0016	1.765	6	
2−	1.732	1312	1.707	0	
		$20\overline{14}$	1.707	0	
2	1.679	$13\overline{14}$	1.656	302	2.5
		2012	1.656	151	
		0018	1.569	34	
1	1.575	1314	1.559	69	0.5
		$20\overline{16}$	1.558	34	

TABLE 4—*Continued*

Observations (Pabst)		Ideal vermiculite (Gruner)			Average of observations on 6 vermiculites (Gruner)
Intensity	Spacing	Indices	Spacing	Intensity	Intensity
		060	1.533	205	
		$33\bar{2}$	1.533	412	
9	1.533	330	1.524	250	4
		$33\bar{4}$	1.524	164	
		$13\overline{16}$	1.513	214	
		2014	1.513	108	
		332	1.498	35	0.5
		$33\bar{6}$	1.498	36	
2−	1.448	1316	1.428	405	1.5
		$20\overline{18}$	1.428	203	
		0020	1.412	62	1
		$13\overline{18}$	1.389	0	
		2016	1.389	0	
1	1.358	338	1.347	67	0.5
		$33\overline{12}$	1.347	61	
2	1.329	1318	1.314	405	2.5
4	1.321	$20\overline{20}$	1.314	204	
2	1.292	0022	1.284	58	1
2+	1.268				
1+	1.167				
1	1.127				
1	1.082				
2	1.048				
$d_{001}=28.46$			$d_{001}=28.24$		

significant loss occurs due to the lag attendant upon the necessarily rapid heating rate.

The vermiculite curve (C) shows two prominent breaks at rather low temperature which correspond to the loss of a large part of the water. After this loss the structure is more or less like that of talc, according to Gruner,[8] and a further break corresponding to the high temperature water loss of that mineral is to be expected. It seems, however, that in the present case at least this further water loss occurs at a slightly lower temperature than for true talc.

The curve for hydrobiotite (B) was run on the well-known material from Libby, Montana, which is commonly called "vermiculite" and whose remarkable exfoliation has led to its commercial use. It has a

[8] *Op. cit.*

water content of 11 per cent and a specific gravity of 2.64, intermediate between vermiculite and biotite. Such material is called hydrobiotite by Gruner.[9] Presumably its structure, as well as its composition, is intermediate between that of true vermiculite and biotite. This is in harmony with its thermal behavior. The low temperature breaks in the curve are less conspicuous than in vermiculite because there is less water to lose and the high temperature break is scarcely discernible because the structure is about one half like biotite which shows no breaks.

Powder diffraction patterns of the vermiculite and of the partly dehydrated material were made with molybdenum radiation and an 8 inch cassette. Observations on these two patterns are shown in Tables 4 and 5 in comparison with the results of Gruner. This leaves no doubt that the differential thermal curves, discussed above, really record the changes

Table 5. Powder Pattern of Vermiculite from Humphreys, California After Removal of About 15% Water

Vermiculite		Talc (after Gruner)		
Intensity	Spacing	Indices	Spacing	Intensity
6*	9.23	002	9.260	4†
7	4.57	6 planes	4.53 4.41	3 b
		6 planes	3.83	1 v.b.
6	3.044	006	3.086	5
9 b	2.63	$20\bar{2}$, 130 $13\bar{2}$, 200	2.613 2.578	1 b
9	2.473	$20\bar{4}$, 132	2.447	5
3	2.200	$20\bar{6}$, 134	2.178	2
4	2.099	$13\bar{6}$, 204	2.089	1
4	1.904	$20\bar{8}$, 136	1.897	0.5
2	1.732			
3	1.646	138 $20\overline{10}$	1.663 1.647	3 b 2 b
8	1.539	060, $33\bar{2}$	1.517	4
2	1.513	330, 062, $33\bar{4}$	1.499	1
			1.453	1
			1.440	0.5
5	1.374	$13\overline{12}$, 2010	1.384	4 b
2	1.324			
3	1.304	260	1.307	1
1	1.281	$26\bar{4}$, 400	1.289	2 b

* Mo radiation.
† Fe radiation.

[9] *Op. cit.*

Gruner postulated for vermiculite. Some of the spacings observed for vermiculite are slightly larger than those given for the ideal material, but this is due at least in part to the fact that real vermiculite always has a slightly larger c dimension than the ideal.

The intensity differences between the partly dehydrated vermiculite and talc shown in Table 5 are due in some measure to the fact that different radiation was used in the two cases, introducing a difference in the effect of the glancing angle. In any case exact correspondence cannot be expected. There is much variation in detail among the seven patterns of this sort tabulated by Gruner, but four of them show a line at or near the position for a spacing of 1.732Å which does not correspond to any line tabulated for talc.

Chlorite. For the most part the micaceous crust of the nodules is composed of chlorite. Generally this mineral, like the vermiculite, forms a crust of flakes parallel to the nodule surface, but in a few spots the chlorite plates show a haphazard arrangement as in Fig. 2. Chlorite is also a minor constituent of the inner zones. In these it occurs mostly in the talc-rich parts and forms aureoles or pressure-shadows about or among magnetite grains.

The properties of the encrusting chlorite were examined in detail on some material obtained from a thick portion of the crust consisting entirely of chlorite. A powder pattern of this can be fully interpreted after McMurchy[10] and shows no unusual features.

G (Berman balance) = 2.63
Optically negative, very low birefringence
$\beta = 1.580 \pm 0.003$
$2V =$ ca. 5°
Weakly pleochroic, pale dirty green to colorless
Ignition loss = 9.8%

These are the properties of clinochlore. Checks on the optical properties of the encrusting chlorite in half a dozen other specimens show that much of it has a slightly lower index, is nearly uniaxial, some negative, so that the composition is variable and lies in the range of penninite to clinochlore.

Tremolite. A layer of brittle, glassy, prisms of greenish amphibole underlies the micaceous crust in many specimens. The thickness of this layer ranges to about 6 mm. In some specimens it is very sharply defined with an excellent orientation of the crystals, as seen in Fig. 1, in others the amphibole crystals extend into the lower part of the micaceous crust and where the crust is coarse the distinctness of the layer is lost.

Some of the properties of this amphibole are:—

Brittle, perfect cleavage
$\beta = 1.626 \pm 0.003$, moderate birefringence
Optically negative
$2V =$ ca. 80° (Universal stage)
$Z \wedge c = 18°$ (Universal stage)
Pleochroism very weak
Z pale green
X and Y nearly colorless

[10] McMurchy, R. C., The crystal structure of the chlorite minerals: *Zeits. Krist.*, **88**, 420–432 (1934).

These properties were determined on material taken from the specimen that yielded the vermiculite which was studied in detail. They indicate a tremolite with some slight iron content, tending towards actinolite. Tremolite in other specimens showed practically the same properties.

Occasional ragged grains of this mineral are scattered through the lower zones.

Anthophyllite. This mineral makes up the major part of the radial zone. It occurs in soft colorless fibers, which attain a length of half a centimeter or more. In general, no single fiber extends through the entire thickness of the radial zone, which consists of many tufts and slightly divergent sheaves of anthophyllite. Some of the properties of the mineral are:—

$\beta = 1.635 \pm 0.003$, moderate birefringence
$Z \wedge c = 0°$ (Universal stage)
Colorless

This is evidently an orthorhombic amphibole with moderate iron or aluminum content and may be properly called anthophyllite. Megascopically it has the typical appearance of this mineral.

Talc. This mineral is the most abundant constituent of the altered zones surrounding the serpentine nodules. Felted masses of minute talc plates or flakes make up the innermost zone which immediately overlies the serpentine. A similar zone occurs just under the micaceous crust or the tremolite zone in some cases. Talc is also interspersed with the anthophyllite of the radial zone in varying amount. A part of this talc is fibrous and in some spots this zone is largely composed of such talc. The total thickness of talc, partly fibrous and partly felted, reaches a maximum of over 6 centimeters in the specimen from which section I in table 3 was taken.

A small amount of talc occurs as a replacement of tremolite. This can be seen very clearly in several specimens in which it pseudomorphs idiomorphic tremolite projecting into the chlorite crust.

The talc is nearly colorless except where limonite stained or interspersed with grayish chlorite. Its optical properties are those normal for this mineral. It is readily distinguished from the amphiboles by its lower refraction and from the chlorite and vermiculite by its higher birefringence so that its distribution and texture can be seen with ease.

Minor constituents. Magnetite occurs in scattered grains in most specimens. It may appear in any zone and its distribution is most irregular. A very small amount of biotite was observed in the micaceous crust in one thin section and a bit of hornblende was seen just under the crust in another, but these constituents are not even discernible megascopically and are certainly not characteristic of the nodules. A little limonite stain tends to emphasize the zoning in some cases.

Conclusion

It is now possible to reinterpret the analyses. The analysis given in Table 2 certainly represents a part of the crust that is mostly vermiculite. Three bromoform separations of the encrusting vermiculite were made in the course of this work. The contamination with tremolite was found by weighing of clean concentrates to be 13, 29 and 39 per cent. It seems

likely that most of the lime of this analysis is due to such contamination.

The analysis given in Table 1, of the "outer part of radial talc-actinolite zone," is clearly an analysis of a material rich in anthophyllite. From this MacDonald calculated what he called the "composition of actinolite," presumably using his estimate of the mineral composition of this zone. In view of the presence of two distinct amphiboles, and because of local variations in the mineralogy of the zones, this calculation has limited value. It may well be that the anthophyllite contains a lower proportion of calcium than shown in this analysis and that the calcium content is again due to the presence of a small amount of tremolite.

There is too much variation in the zone succession to allow any general statement of the sequence of changes. Nevertheless, a few points appear very clearly. Some transfer of material occurred in the formation of these zones. The amount and nature of this transfer was at least partly determined by very sharply localized conditions.

Little, if any, transfer of alkalies occurred. The small content of potash and soda shown in Table 2 may be contained in the vermiculite which is *not* the principal encrusting mineral, or may be partly in the tremolite of the crust. It seems certain that the more common, chloritic parts of the crust are even lower in alkalies.

Calcium reaches a maximum concentration in the tremolite zone *just* under the micaceous crust and, though no analysis of this exists, it is certain that this concentration greatly exceeds that shown in Table 1 or in MacDonald's Fig. 3. This maximum is reached in a narrow zone which lies between two zones very low in calcium, but this thin tremolite layer is discontinuous or wholly lacking around some nodules.

A few details of the order of crystallization can be given. The pseudomorphs of tremolite after talc in the outer parts suggest that the talc may have formed over a longer interval than some of the other constituents, possibly in several stages, and that the concentration of calcium in a narrow zone was reversed at a late stage. There is nothing to indicate that all of the talc is a replacing mineral.

It may be that the scattered magnetite is a relic embedded in all parts of the zones. It is anhedral, in clusters or remnants of broken or altered grains. Structures in the chlorite crust suggest crystallization locally influenced by preexistent grains of magnetite. Excellent pressure shadows (see Fig. 2) of chlorite occur about the magnetite of the inner zones and show very clearly that this chlorite formed *after* the adjoining talc or anthophyllite.

These observations still leave the story of the formation of the zoned nodules very incomplete, but one suggestion may not be amiss. It is that mineral occurrences of this sort can be most effectively studied by

methods analogous to those that have been used with much success in the study of pegmatites, modified, of course, to suit the much finer grain of the material. As in pegmatites, it is practically impossible to get satisfactory bulk compositions of the whole or of typical parts. The history of the assemblage is best arrived at by a careful identification of all discernible minerals, the analysis of those whose composition may be especially significant, and the determination of such fragments of the sequence of crystallization as may be recognizable. Just as one would not describe a pegmatite from hand specimens, however numerous, but would examine the whole body, one must examine specimens or sections in which the structure and relations of the whole assemblage are adequately shown.

Acknowledgments

The writer wishes to thank Dr. J. B. Page of the Division of Soils and Mr. W. H. Dore of the Division of Plant Nutrition, University of California, for the preparation of the differential thermal curves and the x-ray patterns used in this study. A grant from the Committee on Research of the University of California in support of this work is gratefully acknowledged.

SAMPLEITE, A NEW MINERAL FROM CHUQUICAMATA, CHILE

C. S. Hurlbut, Jr., *Harvard University, Cambridge, Mass.**

Abstract

Sampleite is found characteristically in crusts; small platy crystals give poor crystallographic measurements. Orthorhombic; dipyramidal—$2/m2/m2/m$. $a_0=9.70$ Å, $b_0=38.40$ Å, $c_0=9.65$ Å. $a_0:b_0:c_0=0.2526:1:0.2513$. Cleavage: {010} perfect, {100} and {001} good. H.=5, G.=3.20. Color: light blue-green in crystals, light blue in crusts. Opt.: (−), $2V=5°-20°$, $r>v$, $X=b=1.629$—deep blue, $Y=a=1.677$—light blue, $Z=c=1.679$—colorless. Chemical formula—$8[NaCaCu_5(PO_4)_4Cl \cdot 5H_2O]$. Named after Mr. Mat Sample of the Chile Exploration Company, Chuquicamata, Chile.

Early in 1940 the Chile Exploration Company sent to the Department of Mineralogy of Harvard University a number of specimens of several unidentified minerals from its mine at Chuquicamata, Chile. One of these minerals, a copper iodate, studied by Berman and Wolfe in 1940[1] proved to be a new mineral and was named *bellingerite*. A blue and green platy mineral still remained unidentified and there was insufficient material to carry out a complete study. About one year later more specimens of this mineral were received and the writer undertook the separation and purification of a sample for chemical analysis. The Chile Exploration Company kindly offered to make the analysis in their chemical laboratory. This analysis was incomplete because of an inadequate sample. It was not until April 1941 when a sufficiently larger amount of material was received that a complete analysis was made by F. A. Gonyer.

This mineral is named *sampleite* after Mr. Mat Sample, Assistant General Manager of the Chile Exploration Company at Chuquicamata, Chile. The name seems most fitting because of Mr. Sample's interest and assistance in the mineralogical work carried out by members of the geologic staff during the many years he was Mine Superintendent at Chuquicamata.

Occurrence

Mr. Lester G. Zeihen of the Chile Exploration Company, who found the mineral, gives the following information on its occurrence: Sampleite was first noted on the northwest ends of benches C-3, D-1, and D-2 as earthy crusts and crack fillings associated with gypsum, atacamite, jarosite and limonite in a highly sericitized rock. Later it was observed near the southeast ends of benches C-3, D-1, D-2 and E-1, where it oc-

* Contributions from the Department of Mineralogy and Petrography, Harvard University, No. 254.

[1] Berman, H., and Wolfe, C. W., Bellingerite, a new mineral from Chuquicamata, Chile: *Am. Mineral.*, **25**, 505–512 (1940).

curs as micaceous rosettes and aggregates of small platy individual crystals in small cracks. Here it is commonly associated with dendrites of manganese and iron oxides, gypsum, specular hematite, and libethenite in sericitized and kaolinized quartz monzonite and granodiorite. Ultimately it was found to be not uncommon in the higher inactive benches of the mine especially on the east side of bench B-2, where it is associated with limonite and atacamite in a quartz monzonite, and has a micaceous appearance. In all the occurrences mentioned above sampleite is present under highly oxidized near-surface conditions. It appears to be the most recent mineral deposited with the exception of gypsum.

Crystallography

Morphology. The available crystals of sampleite are exceedingly thin, flattened on (010). Although the tabular nature is evident in the drawing, its thickness is relatively greater than that of the crystal so that the terminating faces can be more readily shown. The average crystal dimensions are 0.3 mm. × 0.2 mm. × 0.03 mm. Sampleite is pseudotetragonal with the *b* crystal axis corresponding to the pseudotetragonal axis *c*. When lying on the dominant *b* face, the crystals have a square outline with the *p* faces truncating at approximately 45°. This pseudotetragonal symmetry is also shown in the optical properties and in the unit cell dimensions.

Goniometric measurements were poor and only approximate angular readings could be made. Most of the faces are present on the crystals as fine lines, while the pyramid *p* shows only as tiny points. Form *b*{010} is the only one that gives good reflections. The measurements made on five crystals are given below in Table 1. The elements given were obtained from *x*-ray measurements, since they appear more reliable than those obtained from morphological data.

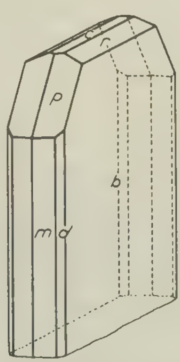

Fig. 1. Sampleite

TABLE 1. SAMPLEITE: ANGLE-TABLE

Orthorhombic; dipyramidal—$2/m\ 2/m\ 2/m$

$a_0:b_0:c_0=0.2526:1:0.2513$; $p_0:q_0:r_0=0.9948:0.2513:1$

$q_1:r_1:p_1=0.2526:1.0052:1$; $r_2:p_2:q_2=3.9794:3.9587:1$

	Goniometric Measurements			Calculated using structural elements	
Forms	No. of faces	ϕ	ρ	ϕ	ρ
c 001	3	—	0°	—	0°00′
b 010	10	0°	90	0°00′	90 00
m 110	5	77	90	75 49	90 00
d 150	4	39	90	38 22	90 00
r 021	10	0	25½	0 00	26 41
p 111	7	77	45½	75 49	45 44

X-Ray Crystallography. A rotation photograph and zero and first-layer line Weissenberg photographs were taken with $c[001]$ the axis of rotation. The absolute dimensions of the axes are:

$$a_0=9.70\ \text{Å},\ b_0=38.40\ \text{Å},\ c_0=9.65\ \text{Å}$$

The ratios of these dimensions, $a_0:b_0:c_0=0.2526:1:0.2513$, are believed to be better than the ratios $a:b:c=0.2339:1:0.2319$ as obtained from the morphological measurements.

An x-ray powder picture of sampleite was taken, and the spacings obtained from its measurement are listed below. It is hoped that similar data will be given in descriptions of other new species so that the mineralogist will have one more tool to aid in the identification of the mineral.

I	d	I	d
2	6.798	5	2.588
9	4.345	4	2.420
1	3.893	1	2.177
1	3.569	1	1.930
1	3.237	1	1.801
10	3.073	6	1.710
1	2.800	1	1.440
3	2.693	1	1.373

I = intensity, d = spacing.

PHYSICAL PROPERTIES

Sampleite occurs in platy crystals with a highly perfect cleavage parallel to $b\{010\}$, the platy direction of the crystals. There is also a good cleavage parallel to $a\{100\}$ and $c\{001\}$, thus giving cleavage in the three pinacoidal directions. The hardness is about 4. The specific gravity, determined by suspension in methylene iodide and measurement on a microbalance is 3.20. When in crystals the color is light blue-green. In crusts the color is light blue with a pearly luster. Before the blowpipe sampleite fuses at 2 to a black globule coloring the flame bright green.

Optical Properties

	n-Na		
$X=b$—deep blue	1.629	± 0.001	opt. (−)
$Y=a$—light blue	1.677		$2V=5°–20°$
$Z=c$—colorless	1.679		$r>v$

Chemical Composition

The first sampleite prepared for analysis was sent to the chemical laboratory at Chuquicamata and was analyzed by Mr. F. J. Ojeda. His analysis, given in the following table, is inaccurate because of insufficient material.

Table 2. Sampleite: Chemical Analysis

	1	2	3	4	5	6
CuO	43.2	43.37	44.12	.5545	38.65	40
P_2O_5	29.1	31.55	32.10	.2260	15.76	16
CaO	4.7	5.73	5.83	.1039	8.14	8
MgO	—	.51	.52	.0129		
K_2O	—	1.47	1.49	.0159	4.61	4
Na_2O	1.8	3.06	3.11	.0502		
H_2O	13.5	9.57	9.74	.5409	37.70	40
Cl	tr.	3.89	4.00	.1122	7.82	8
Insol.	3.5	1.48				
		100.67	100.91			
Less O		.89	.91			
		99.78	100.00			
Insol.		1.48				
		98.30				

1. Analysis of sampleite by F. J. Ojeda recalculated in oxides comparable with those in 2.
2. Analysis of sampleite by F. A. Gonyer.
3. Analysis 2 recalculated to 100%.
4. Molecular proportions.
5. Number of oxides in the unit cell, computed by multiplying the values in column 4 by the molecular weight, $M_0=6971$.
6. Ideal cell content.

Content of Unit Cell. The cell volume, 3,594 Å^3, and the measured specific gravity, 3.20, give the molecular weight of the cell contents, $M_0=6971$. Multiplying this value by the molecular proportions, the cell content given in column 5 is found. Assuming the figures given in column 6 to be correct, the unit cell content can be expressed as $Na_8Ca_8Cu_{40}(PO_4)_{32}Cl_8 \cdot 40H_2O$ or $8[NaCaCu_5(PO_4)_4Cl \cdot 5H_2O]$.

A HIGH-INDEX MEDIUM FOR RAPID IMPREGNATION OF FRIABLE MATERIALS

C. P. Kaiser and H. T. U. Smith,
University of Kansas, Lawrence, Kansas.

The need for bonding friable sediments in order to prepare thin sections has long been apparent, and various materials and methods have been proposed for this purpose. Of the impregnating media suggested, balsam has been perhaps most widely employed, and methods for using it have been reviewed by Johannsen,[1] and described by Sayles,[2] Clements,[3] Von Huene,[4] and Waldo and Yuster.[5] Kollolith[6] has about the same index as balsam and is used in much the same way. Bakelite varnish[7] has certain advantages over either of the other two media, and has a higher index (1.60–1.64). All of the above media have a comparatively high viscosity, and it is this factor which hinders their application. Generally, they must be used in some solvent, which necessitates added time to effect thorough impregnation, and special precautions to minimize the formation of bubbles within the specimen when the solvent is evaporated. Good results may be obtained, but the procedure is commonly tedious, and in some cases special equipment is required.

In using aroclor 4465 (index 1.66+)[8] for making heavy mineral mounts the comparatively low viscosity of this material was noted, and the possibility of using it as an impregnating medium suggested itself. Experiments with chalk and with friable sandstone confirmed expectations, and showed that impregnation of materials not too impervious may be effected quickly and effectively by capillary action, without the use of any solvent. In addition to the advantages of speed and simplicity, the high index of the medium provides stronger relief for the common rock

[1] Johannsen, A., *Manual of Petrographic Methods*, McGraw-Hill, New York, 599–602 (1918).

[2] Sayles, R. W., Microscopic sections of till and stratified clay: *Bull. Geol. Soc. Am.*, **32**, 59–62 (1921).

[3] Clements, T., Thin sections of weathered rocks: *Eng. Min. Jour.*, **134**, 99 (1933).

[4] Von Huene, R., A fast and thorough method for impregnating rocks: *Econ. Geol.*, **32**, 387–388 (1937).

[5] Waldo, A. W., and Yuster, S. T., Method of impregnating porous materials to facilitate pore studies: *Bull. Am. Assoc. Petrol. Geol.*, **21**, 259–267 (1937).

[6] Ross, C. S., Methods of preparation of sedimentary materials for study: *Econ. Geol.*, **21**, 454–468 (1926).

[7] Ross, C. S., *op. cit.;* Leggette, M., The preparation of thin sections of friable rock: *Jour. Geol.*, **36**, 549–557 (1928).

[8] Described by Keller, W. D., *Am. Mineral.*, **19**, 384 (1934); obtainable from Monsanto Chemical Co., St. Louis, Mo.

minerals, and is thus particularly suitable for the study of textures. The procedure is briefly described below.

The first step consists in cutting a smooth face on the specimen. This may be done with a diamond disc saw, or with a hack saw, or simply with sand paper, depending on the nature of the material being treated. The resulting face should be as smooth and flat as possible, and any dust or loose grains should be carefully removed. If the material is strong enough, it is desirable to cut a second face parallel to the first, making a slice a few millimeters thick.

A small quantity of aroclor 4465 is next placed in a metal pan or evaporating dish, or simply on a glass slide, and is heated until relatively fluid, which occurs at a temperature somewhat above 120°C. If it is desired to accentuate pore spaces, the red or blue dye used by Waldo and Yuster[9] may be stirred into the molten material. The specimen, previously well dried by heating, is now placed in the liquid aroclor, flat face down, and a constant temperature is maintained until the fluid has been drawn by capillarity into the entire specimen, or into a zone thick enough to permit the grinding of a thin section. During this procedure, the upper surface of the specimen should not be allowed to become immersed in the fluid, as this would retard the escape of air displaced by the fluid, and thus inhibit impregnation.

The process of impregnation appears to be facilitated by wetting with xylol. The specimen may be saturated with xylol before being placed in the melt, or xylol may be added to the free surface of the specimen in the melt before it becomes so hot as to evaporate the liquid more rapidly than it can penetrate downward.

When impregnation is completed, the specimen is removed from the melt and allowed to cool. A thin section may then be prepared by the usual method, except that uncolored aroclor is used to mount the specimen on the glass slide. One step requiring particular care, however, is the mounting of the cover glass. The procedure found best is to place sufficient aroclor for mounting on the cover glass, and to melt it on a hot plate. The slide with its thin section is next warmed by placing it momentarily on the hot plate. The cover glass is then turned over quickly on to the slide with a pair of forceps, and allowed to settle in place. The completed slide is now removed from the hot plate and allowed to cool. No pressure should be exerted on the cover glass, as this may cause the section to break apart. An alternative method of mounting the cover glass is to use balsam in the usual way. This requires less care but takes longer.

[9] *Op. cit.*, pp. 261–262.

A RAPID QUALITATIVE TEST FOR TELLURIUM

HATFIELD GOUDEY,
Jamestown, California

During the investigation of mineralization aureoles in Goldfield, Nevada, a rapid qualitative test for tellurium was desired. The method most commonly used in western mining districts is the addition of a powdered telluride to hot concentrated sulphuric acid, or vice versa. This is quite satisfactory for native tellurium, gold and silver tellurides, but the color reaction is obscured or fails when dealing with goldfieldite ($Cu_6Sb_2(S, Te)_9$), tellurite, durdenite, and emmonsite. I have not had the opportunity of trying its efficacy on the copper tellurides, rickardite and weissite.

The mineral in question in Goldfield was chiefly goldfieldite. Occasional durdenite, tellurite, and native tellurium were encountered megascopically. The textbook method of fusion to sodium telluride was too long when many samples were to be handled. A method involving the solution of the sample and precipitation by sodium thiosulphate was interesting for the apparent differential precipitation of tellurium and selenium but had no practical value for the work at hand and was also too long.

The method finally adopted was very largely suggested by Mr. Roger Downer of Goldfield. A small fragment of the mineral is placed inside and near the rim of a No. 00 porcelain crucible (high form), reclined in a preformed cavity of proper angle in a charcoal block (too often the fragment is lost when the crucible is held in bent tip forceps). The fragment is then gently reduced with a blowpipe flame. Tellurium, if present, forms a lustrous black sublimate round the inside of the crucible. After removing the fragment, the addition of a drop of concentrated sulphuric acid to the now hot crucible confirms the tellurium with the familiar reddish-violet coloration.

Where a number of samples are to be tested at one time, this method is more rapid than the usual one with sulphuric acid, as grinding of the fragment and heating of the solution are eliminated. Also it can be used on any type of tellurium mineral. The test can be made roughly quantitative with practice in judging the relation of the size of the sublimate to the size of the fragment. In a well equipped laboratory refinements in apparatus may be attained but the simple materials described here are the most dependably available at the mine.

PROCEEDINGS OF SOCIETIES

NEW YORK MINERALOGICAL CLUB, INC.

Meeting of January 21, 1942

Dr. Frank L. Hess of the U. S. Bureau of Mines spoke on "Rare Alkalies in New England." After discussing the history of the discoveries of lithium, rubidium, and cesium, a description of pegmatite paragenesis was given. The non-pegmatite occurrences of rare alkalies in New England seem to be limited to lithium in cryophyllite at Rockport, Mass., and a rubidium-bearing phlogopite from Rutland, Vermont. As possible commercial sources of lithium small deposits of spodumene at Warren and Plumbago Mt. in Maine, Leominster, Mass., and Goshen, Conn., were mentioned, as well as lepidolite from near Cobalt, Conn., triphyllite at Newry, Maine, and Grafton, N. H., and amblygonite at Newry. Pollucite could again be mined for its cesium at Hebron and Buckfield, Maine, while a microcline from Hebron, Maine, offers the most promising source of rubidium in the district.

Meeting of February 18, 1942

Mr. Joseph D'Agostino of the Radio Corporation of America spoke on "Quartz and Piezo-Electric Quartz crystals," discussing the following phases of the subject: the phenomenon of piezo electricity, occurrence and mining of high grade quartz in Brazil; testing and selection of crystals for radio use; methods of cutting crystals for frequency control, and the final testing amd mounting of the cut crystals.

Class in Mineralogy. A course of 7 lectures in elementary mineralogy was given for the members during January and February by Dr. Pough. Mr. M. A. Northup and Mr. H. R. Lee assisted with two of the lectures.

Meeting of March 18, 1942

The speaker was Dr. Clifford Frondel of Harvard University whose subject was "Mineral Inclusions." Asterism in phlogopite as caused by oriented inclusions of rutile was discussed at length. Slides of various types of stars were shown, as well as a photo-micrograph of rutile inclusions in phlogopite. Many other instances of mineral inclusions were mentioned and illustrated with slides. Asterism also occurs in such minerals as corundum, rose quartz, and chrysoberyl, and is, as with phlogopite, caused by oriented inclusions of various acicular minerals. A splendid ball of asteriated rose quartz was exhibited.

Meeting of April 15, 1942

The following officers were elected for the coming year:—
President: John N. Trainer; 1st Vice-President: Walter E. Kuenstler; 2nd Vice-President: Dr. Frederick H. Pough; Secretary: M. Allen Northup; Treasurer: James A. Taylor; Directors: Gilman S. Stanton and Ernest Weidhaas.

Professor Paul F. Kerr of Columbia University spoke on his recent trip to South America. A description was given of the Mine of the Honorable Hector Boza in Peru, and of the general features of the Trans-Andean highway. The Chojilla tungsten deposit and the great tin mines at Llallagua in Bolivia were discussed. An account was given of the mineral occurrences at Chuquicamata, Chile, and the nitrate beds of the Maria Elena district. The copper deposit at Sewell in the Andes south of Santiago was also described. The lecture was illustrated with Kodachrome slides and sketch maps.

Meeting of May 20, 1942

The various officers and committee chairmen submitted their annual reports.

Mr. Gilman S. Stanton read a memorial of our late Honorary member, Sir William Henry Bragg.

Mr. Harry Grahl announced that the spring field trip would be held at the Bayliss and Kinkel feldspar quarries in Bedford, N. Y., on Sunday May 24th.

The balance of the meeting was devoted to 10 minute illustrated talks by Dr. Pough, Mr. Karrlson, Mr. Northup, Captain Ehrmann, Mr. Fox and Dr. O'Connell. Mr. Karrlson exhibited splendid specimens of native lead crystals from Långban.

M. A. NORTHUP, *Secretary*

PHILADELPHIA MINERALOGICAL SOCIETY

The Academy of Natural Sciences of Philadelphia, February 6, 1942

A meeting of the Philadelphia Mineralogical society was called to order on the above date by its President, Dr. Hersey Thomas with 53 members and visitors present.

President Thomas introduced the speaker of the evening, Mr. John C. Boyle, Curator of Minerals at the Childrens Museum of Brooklyn, N. Y., whose topic "The Study and Teaching of Mineralogy" was a review of the methods and procedures he developed at the Museum for effective instruction in mineralogy on a level that can be easily understood by the adolescent child.

March 5th, 1942

A meeting of the Philadelphia Mineralogical Society was called to order by the President, Dr. W. Hersey Thomas with 42 members and visitors attending.

Mr. John Cochrane of Bishop & Co. Platinum Works, Malvern, Pa., addressed the meeting. In his talk on "The Platinum Minerals" he gave a historical account of the discovery, use, occurrence, distribution, methods of refining, and present importance of platinum minerals in industry and trade.

April 2, 1942

The April meeting of the Philadelphia Mineralogical Society was held at the Academy of Natural Sciences on April 2nd, 1942, with 65 members and visitors attending this meeting.

Pres. W. Hersey Thomas introduced the speaker of the evening, Dr. Frederich Oldach whose topic "Minerals of French Creek Mine," brought back many pleasant memories of excellent collecting experiences of a number of years ago. His talk included the effect of the intruding magmas into the pre-existing gneiss, shale and calcareous beds, that brought about the mineralization of the French Creek area.

FORREST L. LENKER, *Secretary*